Supporting Information for

Solid-phase synthesis provides a modular, lysine-based platform for fluorescent discrimination of nitroxyl and biological thiols

Andrei Loas, Robert J. Radford, Alexandria Deliz Liang and Stephen J. Lippard*

TABLE OF CONTENTS

Experimental Section

General Methods. Syntheses involving air-sensitive compounds were performed using a double-manifold Schlenk line. Dry inert gas was provided by a zero-grade, in-house nitrogen line. Preparation of samples and solutions requiring strict anaerobic (O_2 < 1 ppm) and water-free (H_2O < 1 ppm) conditions was performed under nitrogen in an inert atmosphere MBraun glove box. Reaction mixtures were monitored by thin-layer chromatography (TLC) on pre-coated, aluminum-backed silica gel 60 F_{254} plates. Gel filtration and flash chromatography were performed on silica gel 60 (230-400 mesh). HPLC separations were carried out at the semi-preparative scale on an Agilent 1200 Series system equipped with multi-wavelength detector and automated fraction collector, using a reverse stationary phase column (Zorbax SB-C18, 5 μm, 9.5 mm × 250 mm). Analytical HPLC was performed on a similar system using a Zorbax SB-C18 reverse stationary phase column (5 μm, 4.6 mm × 250 mm). FT-NMR spectra were acquired at ambient temperature on a Bruker Avance III 400 or a Varian Inova 500 instrument. ^{13}C NMR spectra were acquired with proton decoupling. Assignment of chemical shifts is based on the 1D spectral data. ^{1}H and ^{13}C chemical shifts are reported in ppm relative to $SiMe_4$ (δ = 0.00) and were referenced internally to the residual solvent signals.[1] Low-resolution mass spectra (MS) were acquired on an Agilent 1100 Series LC/MSD Trap spectrometer by electrospray ionization (ESI). The MIT Department of Chemistry Instrumentation Facility acquired high-resolution mass spectra (HRMS) using the ESI technique on a Bruker Daltonics APEXIV 4.7 T FT-ICR-MS instrument. Electronic absorption spectra were collected in absorbance mode on a Varian Cary 50 Bio UV-vis spectrophotometer. Fluorescence spectra were acquired on a Quanta Master 4 L-format scanning spectrofluorimeter (Photon Technology International). The samples for UV-visible and fluorescence spectroscopy were prepared as dilute (1-20 μM) solutions of the analyte in 1.0 cm quartz cuvettes. Melting points were obtained in triplicate using capillary tubes in air with an OptiMelt automated instrument (Stanford Research Systems) and are uncorrected.

Materials. All solvents employed were ACS reagent grade or higher. Rink Amide AM resin (100-200 mesh), Fmoc-Lys(Mtt)-OH, and Boc-Lys(Fmoc)-OH were obtained from EMD Millipore. 2-(7-Aza-1*H*-benzotriazole-1-yl)-1,1,3,3-tetramethyluronium hexafluorophosphate (HATU) was procured from Oakwood Chemicals. *N*,*N*-Diisopropylethylamine (DIPEA, Aldrich) was distilled fresh before use and stored under nitrogen and 3 Å molecular sieves in a Schlenk

flask. Iodoacetic acid *N*-hydroxysuccinimide ester,[2] ethyl (2-methyl-8-aminoquinolin-6-yloxy)acetate,[3] 4',5'-fluoresceindicarboxaldehyde,[4] 5-carboxytetramethylrhodamine (5-CO_2H-TAMRA),[5] and 3',6'-diacetyl-2',7'-dichloro-5-carboxyfluorescein (5-CO_2H-FL)[6] were prepared as previously described. The ligand for the cell-trappable, NO-selective probe Cu_2FL2E was synthesized by a modified procedure,[7] as detailed below. All other solvents and reagents were purchased from commercial sources and used as received.

Scheme S1. Synthesis of FL2E

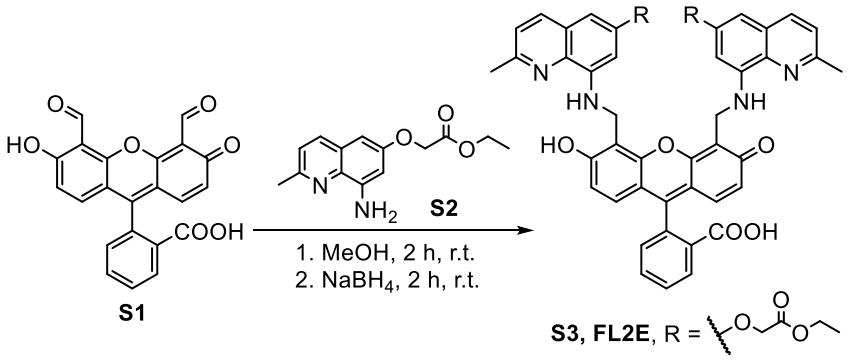

Synthesis of 2-(4,5-Bis((6-(2-ethoxy-2-oxoethoxy)-2-methylquinolin-8-ylamino)methyl)-6-hydroxy-3-oxo-3*H*-xanthen-9-yl)benzoic acid (S3, FL2E). 4',5'-Fluoresceindicarboxaldehyde (**S1**, 80 mg, 206 μmol) and ethyl (2-methyl-8-aminoquinolin-6-yloxy)acetate (**S2**, 120 mg, 462 μmol) were suspended in 25 mL of anhydrous methanol and stirred at room temperature under nitrogen for 2 h. Sodium borohydride (40 mg, 1.0 mmol) was then added in two portions over 5 min to the cloudy red suspension under a nitrogen stream. The reaction mixture clarified to a dark red solution, which was stirred for 2 h at room temperature. The reaction was then quenched by addition of 25 mL of deionized water, and the methanol was removed under reduced pressure. The aqueous phase was saturated with brine and carefully extracted with DCM (4 × 50 mL). The combined organic layers were concentrated to dryness under reduced pressure to give a crude solid, which was brought up in 20 mL of DCM and purified by wet-loading flash chromatography on silica gel (DCM/MeOH = 99:1 to 95:5 v/v), followed by gel filtration through a silica gel layer with DCM/MeOH = 96:4 v/v to afford pure FL2E as an orange-red solid in 23% yield (41.5 mg). Spectroscopic data matched previously reported values.[7]

Scheme S2. Synthesis of Compound **S8**

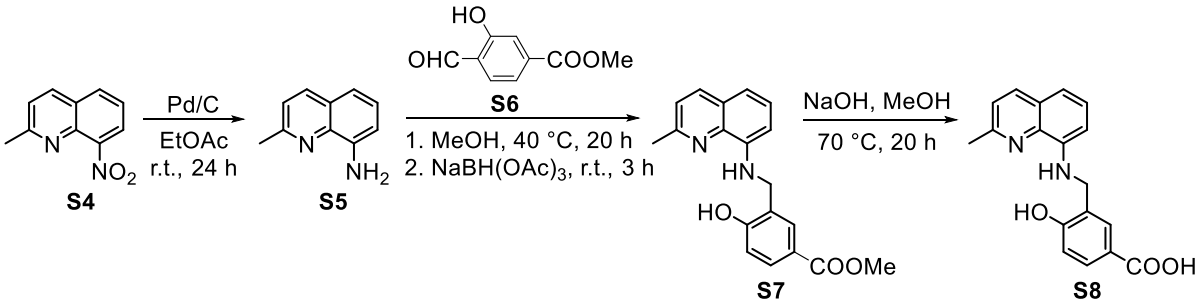

Synthesis of 8-Aminoquinaldine (S5). In a Schlenk flask, 8-nitroquinaldine (**S4**, 0.57 g, 3.0 mmol) and Pd/C catalyst powder moistened with ~50% water (0.2 g, 0.1 mmol Pd equiv) were suspended in 40 mL of ethyl acetate under nitrogen. The flask was degassed by three vacuum/nitrogen cycles and a ~1 atm hydrogen balloon was connected under positive nitrogen pressure. Hydrogen was admitted to the flask and allowed to react overnight with stirring at room temperature. The flask was then evacuated, the catalyst was filtered through a bed of celite, the celite layer was washed with 40 mL of ethyl acetate, and the organic filtrate concentrated to dryness under reduced pressure to afford pure **S5** as a pale yellow powder in >99% yield (0.47 g). ^{1}H NMR (400 MHz, $CDCl_3$): δ 7.95 (d, J = 8.3 Hz, 1H, Ar-*H*), 7.29 (t, J = 7.7 Hz, 1H, Ar-*H*), 7.23 (d, J = 8.3 Hz, 1H, Ar-*H*), 7.13 (dd, J = 8.1, 1.2 Hz, 1H, Ar-*H*), 6.91 (dd, J = 7.4, 1.2 Hz, 1H, Ar-*H*), 5.00 (br, 2H, Ar-NH_2), 2.74 (s, 3H, CH_3); ^{13}C {^{1}H} NMR (100 MHz, $CDCl_3$): δ 156.1, 143.5, 137.9, 136.1, 126.9, 126.35, 122.1, 115.9, 110.1, 25.2; MS (ESI+): *m/z* calcd for $[M + H]^+$ $(C_{10}H_{11}N_2)^+$ 159.1, found 159.0.

Synthesis of Methyl 4-Hydroxy-3-(((2-methylquinolin-8-yl)amino)methyl)benzoate (S7). 8-Aminoquinaldine (**S5**, 0.2 g, 1.26 mmol), methyl 4-formyl-3-hydroxybenzoate (**S6**, 0.18 g, 1.0 mmol), and 1 g of anhydrous sodium sulfate were suspended in 20 mL of anhydrous methanol. A 5 mL volume of chloroform was added to solubilize the entire amount of **S6** and the mixture was heated to 40 °C under nitrogen with stirring for 20 h. To the clear dark yellow solution cooled to room temperature, sodium triacetoxyborohydride (0.64 g, 3.0 mmol) was added in two portions over 5 min under a nitrogen stream. The reaction mixture was then kept under nitrogen with stirring for 3 h at room temperature, the insoluble materials were filtered, the methanol was removed under reduced pressure, and the crude orange-brown residue was purified twice by wet-loading flash chromatography on silica gel (DCM/acetone = 39:1 v/v, then DCM/acetone =

100:0 to 99:1 v/v) to collect a yellow solid, which was triturated with 10 mL of pentane/diethyl ether = 3:2 v/v and dried under vacuum to afford pure methyl benzoate **S7** as a pale yellow powder in 53% yield (0.17 g). Mp. 133-136 °C; ^{1}H NMR (400 MHz, $CDCl_3$): δ 9.72 (br, 1H, Ar-O*H*), 8.00 (d, J = 8.3 Hz, 1H, Ar-*H*), 7.95 (m, 2H, Ar-*H*), 7.30 (s, 1H, Ar-*H*), 7.27 (d, J = 8.6 Hz, 1H, Ar-*H*), 7.27 (td, J = 8.2, 1.5 Hz, 1H, Ar-*H*), 6.95 (dd, J = 7.3, 1.5 Hz, 1H, Ar-*H*), 6.92 (d, J = 8.3 Hz, 1H, Ar-*H*), 6.45 (br, 1H, Ar-N*H*), 4.65 (d, J = 4.7 Hz, 2H, Ar-CH_2), 3.91 (s, 3H, Ar-COOCH_3), 2.71 (s, 3H, Ar-CH_3); ^{13}C {^{1}H} NMR (100 MHz, $CDCl_3$): δ 167.1, 161.8, 157.1, 143.8, 138.9, 136.5, 131.1, 130.6, 126.65, 126.3, 123.4, 122.7, 121.9, 118.6, 116.7, 110.9, 52.0, 49.1, 25.2; MS (ESI+): *m/z* calcd for $[M + H]^+$ $(C_{19}H_{19}N_2O_3)^+$ 323.1, found 323.2.

Synthesis of 4-Hydroxy-3-(((2-methylquinolin-8-yl)amino)methyl)benzoic Acid (S8). Solid **S7** (0.15 g, 0.47 mmol) was dissolved in a mixture of 3 mL of methanol, 4 mL of water, and 1 mL of 33 wt% aq NaOH, and heated to 70 °C with stirring for 20 h. The solution was cooled to room temperature and brought to pH ~3 by dropwise addition of conc. aq HCl. An orange precipitate formed, which was filtered and washed with 20 mL of cold ~1 M aq HCl. A second product crop precipitated from the filtrate, which was filtered, combined with the first crop and washed with 20 mL of water. Drying under air suction overnight, then to constant weight at 60 °C in vacuo afforded benzoic acid **S8** as an orange powder in 83% yield (0.12 g). Mp. 184-186 °C; ^{1}H NMR (500 MHz, $CD_3OD/CDCl_3$ = 4:1 with a drop of $(CD_3)_2SO$): δ 8.21 (d, J = 8.1 Hz, 1H, Ar-*H*), 7.99 (s, 1H, Ar-*H*), 7.82 (d, J = 8.1 Hz, 1H, Ar-*H*), 7.43 (d, J = 8.1 Hz, 1H, Ar-*H*), 7.36 (t, J = 7.6 Hz, 1H, Ar-*H*), 7.17 (d, J = 8.1 Hz, 1H, Ar-*H*), 6.88 (d, J = 8.1 Hz, 1H, Ar-*H*), 6.85 (d, J = 7.6 Hz, 1H, Ar-*H*), 4.56 (s, 2H, Ar-CH_2), 2.76 (s, 3H, Ar-CH_3); ^{13}C {^{1}H} NMR (125 MHz, $CD_3OD/CDCl_3$ = 4:1 with a drop of $(CD_3)_2SO$): δ 169.8, 161.2, 157.1, 143.05, 140.0, 132.1, 131.8, 128.5, 128.4, 125.8, 123.4 (overlap), 122.55, 116.6, 115.6, 109.7, 44.0, 24.0; HRMS (ESI+): *m/z* calcd for $[M + H]^+$ $(C_{18}H_{17}N_2O_3)^+$ 309.1239, found 309.1247.

Scheme S3. Synthesis of CLT and CuCLT

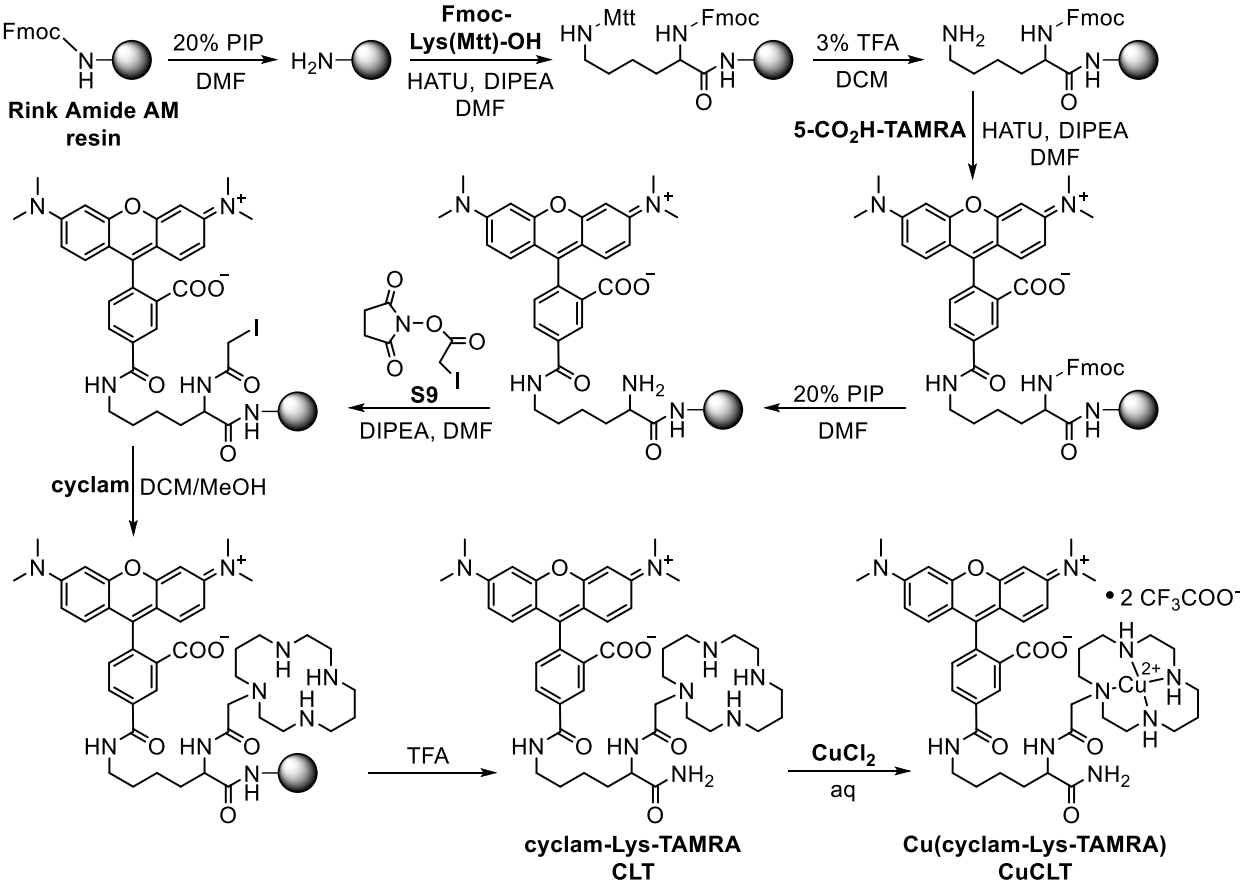

Abbreviations: Fmoc = fluorenylmethyloxycarbonyl, Mtt = 4-methyltrityl, PIP = piperidine, TFA = trifluoroacetic acid

Synthesis of Cyclam-Lys-TAMRA (CLT). Rink Amide AM resin (134 mg, 0.74 mmol/g, 100 μmol) was placed in a 20 mL peptide synthesis reaction vessel and swelled by stirring in 4 mL of anhydrous DMF for 30 min prior to synthesis. The protecting Fmoc group of the resin was removed by stirring with 2 mL of a 20% (v/v) solution of piperidine in DMF for 15 min, followed by washing with 5 × 2 mL of DMF. Next, Fmoc-Lys(Mtt)-OH (250 mg, 400 μmol, 4 equiv) and HATU (152 mg, 400 μmol, 4 equiv) were dissolved in 2 mL of a 10% (v/v) solution of DIPEA in DMF and added to the reaction vessel with stirring. After 30 min, the resin was washed with 5 × 2 mL of DMF and the Mtt group was removed from the ε-terminal Lys(Mtt) residue by stirring with 2 × 4 mL of a 3% (v/v) solution of TFA in DCM for 2 × 10 min. After washing the resin with 5 × 2 mL of DMF, a pre-activated (5 min) solution of 5-CO_2H-TAMRA (130 mg, 300 μmol, 3 equiv) and HATU (114 mg, 300 μmol, 3 equiv) in 3 mL of 10% (v/v) DIPEA in DMF was added to the reaction vessel and the mixture was kept at room temperature

with stirring for 3 h. The resin was then washed with 5 × 2 mL of DMF and the N-terminal Fmoc protecting group of the Fmoc-Lys residue was removed by treating the resin with 2 mL of a 20% (v/v) solution of piperidine in DMF for 15 min, followed by another wash with 5 × 2 mL of DMF. Next, iodoacetic acid *N*-hydroxysuccinimide ester (**S9**, 88 mg, 300 μmol, 3 equiv) was dissolved in 2 mL of a 1% (v/v) solution of DIPEA in DMF, placed in the reaction vessel and allowed to react with stirring for 60 min. Lastly, the resin was washed with 5 × 2 mL of DMF and 4 mL of a solution of cyclam (60 mg, 300 μmol, 3 equiv) in 5% (v/v) methanol in DCM was placed in the reaction vessel and allowed to react with stirring overnight. The resulting crude resin was washed with 5 × 2 mL of methanol, 5 × 2 mL of DMF, and 5 × 2 mL of DCM. The cyclam-Lys-TAMRA construct (CLT) was cleaved from the resin by treatment with a TFA/water/triisopropylsilane 95:2.5:2.5 (v/v/v) solution for 90 min, followed by washing the resin with 2 × 2 mL of acetonitrile and concentrating the combined organic filtrates to dryness. The crude purple solid was purified by semi-preparative reverse phase HPLC using the (A) water (0.1% v/v TFA) / (B) CH_3CN (0.1% v/v TFA) solvent system, according to the following protocol: constant flow rate 3 mL min^{-1}; 5 min, isocratic flow 10% B; 5 min, linear gradient 10-22% B; 20 min, linear gradient 22-35% B. The equivalent fractions from independent runs were combined and lyophilized to afford CLT as a purple powder in 21% yield (19.5 mg). The purity was judged to be ~98% by analytical HPLC (Figure S15A), employing the solvent system above according to the following protocol: constant flow rate 1 mL min^{-1}; 5 min, isocratic flow 10% B; 30 min, linear gradient 10-50% B; retention time: 23.2 min. ^{1}H NMR (400 MHz, CD_3OD): δ 8.95 (t, J = 5.7 Hz, 1H, Ar-CON*H*), 8.78 (d, J = 2.1 Hz, 1H, Ar-*H*), 8.57 (d, J = 5.6 Hz, 1H, Lys-N*H*CO), 8.27 (dd, J = 8.1, 2.0 Hz, 1H, Ar-*H*), 7.54 (d, J = 8.1 Hz, 1H, Ar-*H*), 7.14 (d, J = 9.4 Hz, 2H, Ar-*H*), 7.06 (dd, J = 9.5, 2.6 Hz, 2H, Ar-*H*), 6.99 (d, J = 2.6 Hz, 2H, Ar-*H*), 4.23 (br, 1H, Lys-C*H*), 3.67 (br, 2H, Lys-NHCO-CH_2), 3.50 (t, J = 6.1 Hz, 2H, Lys-CH_2), 3.31 (s, 12H, Ar-N(CH_3)$_2$), 3.30−2.65 (br m, 20H, cyclam-CH_2), 1.84 (m, 2H, Lys-CH_2), 1.75 (m, 2H, Lys-CH_2), 1.58 (m, 2H, Lys-CH_2); MS (ESI+): *m/z* calcd for $[M + H]^+$ $(C_{43}H_{60}O_6N_9)^+$ 798.5, found 798.8; HRMS (ESI−): *m/z* calcd for $[M - H]^-$ $(C_{43}H_{58}O_6N_9)^-$ 796.4510, found 796.4520.

Synthesis of Cu(cyclam-Lys-TAMRA) (CuCLT). Cyclam-Lys-TAMRA (15 mg, 16 μmol) was dissolved in 1.6 mL of aq 0.1 M $CuCl_2$ (160 μmol $CuCl_2$, 10 equiv) and kept at room temperature with stirring overnight. The dark purple solution was purified directly by semi-

preparative reverse phase HPLC using the (A) water (0.1% v/v TFA) / (B) CH_3CN (0.1% v/v TFA) solvent system, according to the following protocol: constant flow rate 3 mL min^{-1}; 5 min, isocratic flow 10% B; 20 min, linear gradient 10-30% B. The equivalent fractions from independent runs were combined and lyophilized to afford the TFA salt of CuCLT as a purple powder in 61% yield (9.5 mg). The purity was judged to be >95% by analytical HPLC (Figure S15B), employing the protocol described for CLT; retention time: 23.1 min. MS (ESI+): *m/z* calcd for $[M + TFA]^+$ $(C_{45}H_{59}O_8N_9F_3Cu)^+$ 973.4, found 973.6; HRMS (ESI+): *m/z* calcd for $[M + TFA]^+$ $(C_{45}H_{59}O_8N_9F_3Cu)^+$ 973.3729, found 973.3716.

Scheme S4. Synthesis of QLT

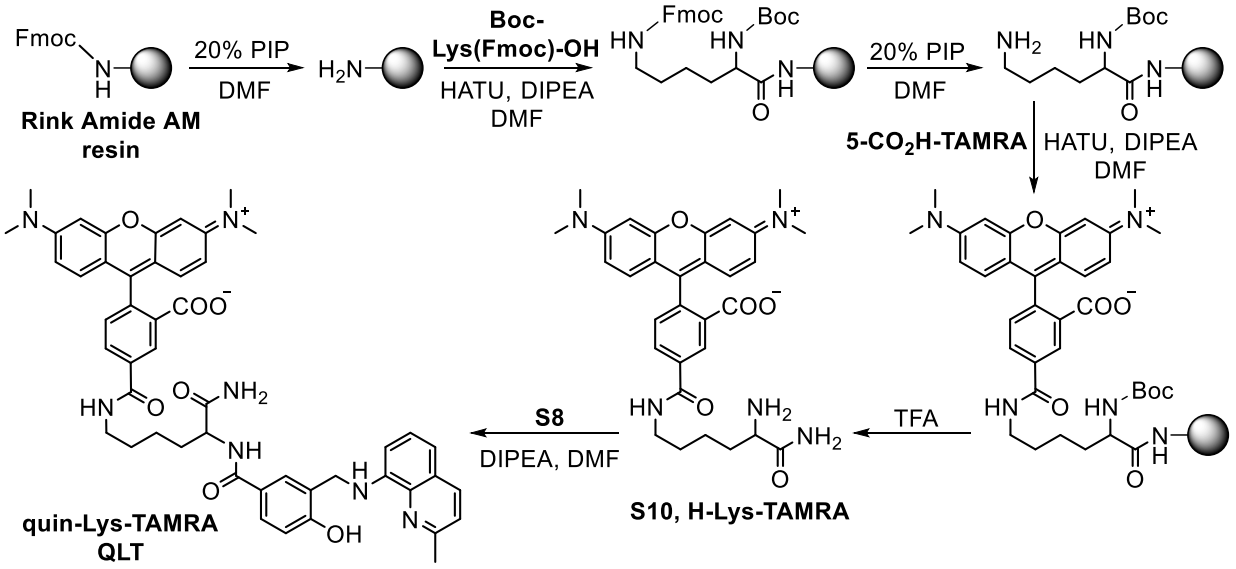

Fmoc = fluorenylmethyloxycarbonyl, Boc = *tert*-butyloxycarbonyl, PIP = piperidine, TFA = trifluoroacetic acid

Synthesis of H-Lys-TAMRA (S10). Rink Amide AM resin (130 mg, 0.77 mmol/g, 100 μmol) was placed in a 20 mL peptide synthesis reaction vessel and swelled by stirring in 4 mL of anhydrous DMF for 30 min prior to synthesis. The protecting Fmoc group of the resin was removed by stirring with 2 mL of a 20% (v/v) solution of piperidine in DMF for 15 min, followed by washing with 5 × 2 mL of DMF. Next, Boc-Lys(Fmoc)-OH (130 mg, 280 μmol, 2.8 equiv) and HATU (104 mg, 280 μmol, 2.8 equiv) were dissolved in 2 mL of a 10% (v/v) solution of DIPEA in DMF and added to the reaction vessel with stirring. After 30 min, the resin was washed with 5 × 2 mL of DMF and a pre-activated (5 min) solution of 5-CO_2H-TAMRA (130 mg, 300 μmol, 3 equiv) and HATU (114 mg, 300 μmol, 3 equiv) in 4 mL of 10% (v/v) DIPEA in

DMF was added to the reaction vessel and the mixture was kept at room temperature with stirring for 3 h. The resin was then washed with 8 × 2 mL of DMF. The N-terminal Boc protecting group of the lysine residue was removed upon cleavage of the H-Lys-TAMRA construct from the resin by treatment with a TFA/water/triisopropylsilane 95:2.5:2.5 (v/v/v) solution for 90 min, followed by washing the resin with 2 × 2 mL of acetonitrile and concentrating the combined organic filtrates to dryness. The crude purple solid was purified by semi-preparative reverse phase HPLC using the (A) water (0.1% v/v TFA) / (B) CH_3CN (0.1% v/v TFA) solvent system, according to the following protocol: constant flow rate 3 mL min^{-1}; 5 min, isocratic flow 15% B; 20 min, linear gradient 15-40% B; retention time: 12.9 min. The equivalent fractions from independent runs were combined and lyophilized to afford H-Lys-TAMRA (**S10**) as a purple powder in 24% yield (19 mg). ^{1}H NMR (500 MHz, CD_2Cl_2/CD_3OD = 9:1): δ 8.75 (s, 1H, Ar-*H*), 8.26 (d, *J* = 7.5 Hz, 1H, Ar-*H*), 7.36 (d, *J* = 7.5 Hz, 1H, Ar-*H*), 7.11 (d, *J* = 8.7 Hz, 2H, Ar-*H*), 6.88 (dd, *J* = 9.0, 2.3 Hz, 2H, Ar-*H*), 6.79 (d, *J* = 2.3 Hz, 2H, Ar-*H*), 3.99 (t, *J* = 5.6 Hz, 1H, Lys-C*H*), 3.47 (t, *J* = 6.1 Hz, 2H, Lys-CH_2), 3.26 (s, 12H, Ar-N(CH_3)$_2$), 1.94 (m, 2H, Lys-CH_2), 1.70 (m, 2H, Lys-CH_2), 1.56 (m, 2H, Lys-CH_2); MS (ESI+): *m/z* calcd for $[M + H]^+$ $(C_{31}H_{36}O_5N_5)^+$ 558.3, found 558.3.

Synthesis of Quin-Lys-TAMRA (QLT). Benzoic acid **S8** (10 mg, 32 μmol) and HATU (12 mg, 32 μmol) were dissolved in 1.5 mL of a 10% (v/v) solution of DIPEA in anhydrous DMF and mixed for 10 min at room temperature. This solution was added to solid H-Lys-TAMRA (**S10**, 13 mg, 20 μmol) and the mixture was kept at room temperature with stirring for 4 h. The reaction was quenched with 20 mL of deionized water and the resulting mixture was lyophilized to give a crude purple solid, which was purified by semi-preparative reverse phase HPLC using the (A) water (0.1% v/v TFA) / (B) CH_3CN (0.1% v/v TFA) solvent system, according to the following protocol: constant flow rate 3 mL min^{-1}; 5 min, isocratic flow 15% B; 25 min, linear gradient 15-35% B. The equivalent fractions from independent runs were combined and lyophilized to afford QLT as a purple powder in 17% yield (3.3 mg). The purity was judged to be ~98% by analytical HPLC (Figure S15C), employing the protocol described for CLT; retention time: 28.2 min. ^{1}H NMR (400 MHz, CD_2Cl_2/CD_3OD = 9:1): δ 8.72 (d, *J* = 1.7 Hz, 1H, Ar-*H*), 8.19 (dd, *J* = 7.9, 1.7 Hz, 1H, Ar-*H*), 8.15 (d, *J* = 9.5 Hz, 1H, Ar-*H*), 7.86 (d, *J* = 2.2 Hz, 1H, Ar-*H*), 7.68 (dd, *J* = 8.3, 2.2 Hz, 1H, Ar-*H*), 7.34 (m, 3H, Ar-*H*), 7.15 (d, *J* = 9.4 Hz, 1H, Ar-*H*),

7.07 (d, J = 9.4 Hz, 2H, Ar-*H*), 6.85 (m, 4H, Ar-*H*), 6.76 (t, J = 2.2 Hz, 2H, Ar-*H*), 4.55 (m, 1H, Lys-C*H*), 4.50 (s, 2H, Ar-CH_2) 3.47 (t, J = 6.6 Hz, 2H, Lys-CH_2), 3.25 (s, 12H, Ar-N(CH_3)$_2$), 2.71 (s, 3H, Ar-CH_3), 1.90 (m, 2H, Lys-CH_2), 1.71 (m, 2H, Lys-CH_2), 1.52 (m, 2H, Lys-CH_2); HRMS (ESI+): *m/z* calcd for $[M + H]^+$ $(C_{49}H_{50}O_7N_7)^+$ 848.3772, found 848.3783.

Scheme S5. Synthesis of QLF

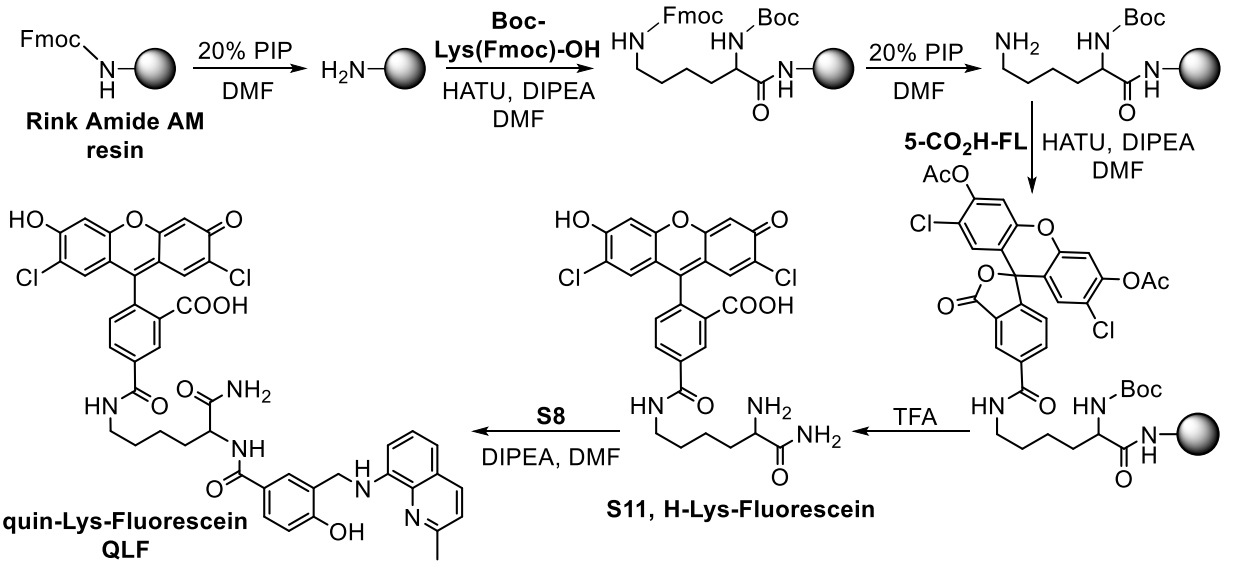

Fmoc = fluorenylmethyloxycarbonyl, Boc = *tert*-butyloxycarbonyl, PIP = piperidine, TFA = trifluoroacetic acid

Synthesis of H-Lys-Fluorescein (S11). H-Lys-Fluorescein (**S11**) was prepared in a similar manner to H-Lys-TAMRA (**S10**) on the 100 μmol scale, using 3',6'-diacetyl-2',7'-dichloro-5-carboxyfluorescein (5-CO_2H-FL, 160 mg, 300 μmol, 3 equiv) instead of 5-CO_2H-TAMRA. The construct was purified by semi-preparative reverse phase HPLC using the (A) water (0.1% v/v TFA) / (B) CH_3CN (0.1% v/v TFA) solvent system, according to the following protocol: constant flow rate 3 mL min^{-1}; 5 min, isocratic flow 25% B; 30 min, linear gradient 25-60% B; retention time: 14.1 min. The equivalent fractions from independent runs were combined and lyophilized to afford H-Lys-Fluorescein (**S11**) as a yellow powder in 6% yield (3.5 mg). The mono-acetylated analogue of **S11** was also isolated in 3% yield (1.7 mg). ^{1}H NMR (400 MHz, $(CD_3)_2CO$): δ 8.49 (s, 1H, Ar-*H*), 8.37 (d, J = 7.6 Hz, 1H, Ar-*H*), 7.45 (d, J = 7.6 Hz, 1H, Ar-*H*), 7.06 (s, 2H, Ar-*H*), 6.81 (s, 2H, Ar-*H*), 4.69 (t, J = 7.0 Hz, 1H, Lys-C*H*), 3.52 (m, 2H, Lys-CH_2), 1.76−1.60 (m, 6H, Lys-CH_2); MS (ESI+): *m/z* calcd for $[M + H]^+$ $(C_{27}H_{24}O_7N_3Cl_2)^+$ 572.1, found 572.2.

Synthesis of Quin-Lys-Fluorescein (QLF). Benzoic acid **S8** (3.8 mg, 12 μmol) and HATU (5.0 mg, 12 μmol) were dissolved in 1 mL of a 10% (v/v) solution of DIPEA in anhydrous DMF and mixed for 10 min at room temperature. This solution was added to solid H-Lys-Fluorescein (**S11**, 3.5 mg, 6.2 μmol) and the mixture was kept at room temperature with stirring for 3 h. The reaction was quenched with 5 mL of deionized water and 5 mL of acetonitrile. The mixture was lyophilized to give a crude orange solid, which was purified by semi-preparative reverse phase HPLC using the (A) water (0.1% v/v TFA) / (B) CH_3CN (0.1% v/v TFA) solvent system, according to the following protocol: constant flow rate 3 mL min^{-1}; 5 min, isocratic flow 20% B; 25 min, linear gradient 20-45% B. The equivalent fractions from independent runs were combined and lyophilized to afford QLF as a yellow-orange powder in 30% yield (1.6 mg). The purity was judged to be ~90% by analytical HPLC (Figure S15D), employing the protocol described for CLT; retention time: 37.7 min. ^{1}H NMR (400 MHz, CD_3OD): δ 8.75 (t, J = 5.7 Hz, 1H, Ar-CON*H*), 8.38 (s, 1H, Ar-*H*), 8.37 (m, 1H, Ar-*H*), 8.13 (dd, J = 8.2, 1.4 Hz, 1H, Ar-*H*), 7.90 (d, J = 2.2 Hz, 1H, Ar-*H*), 7.74 (dd, J = 8.5, 2.2 Hz, 1H, Ar-*H*), 7.53 (d, J = 8.4 Hz, 1H, Ar-*H*), 7.43 (t, J = 7.8 Hz, 1H, Ar-*H*), 7.28 (m, 2H, Ar-*H*), 7.01 (d, J = 7.8 Hz, 1H, Ar-*H*), 6.91 (d, J = 8.5 Hz, 1H, Ar-*H*), 6.84 (s, 2H, Ar-*H*), 6.62 (d, J = 2.8 Hz, 2H, Ar-*H*), 4.56 (s, 2H, Ar-CH_2), 4.53 (m, 1H, Lys-C*H*), 3.43 (t, J = 6.2 Hz, 2H, Lys-CH_2), 2.80 (s, 3H, Ar-CH_3), 1.68 (m, 2H, Lys-CH_2), 1.50 (m, 4H, Lys-CH_2); MS (ESI+): *m/z* calcd for $[M + H]^+$ $(C_{45}H_{38}O_9N_5Cl_2)^+$ 864.2, found 864.7.

Spectroscopic Methods. All aqueous solutions were prepared using deionized water with a resistivity of 18.2 MΩ·cm, obtained with a Milli-Q water purification system (Millipore). Piperazine-*N,N'*-bis(2-ethanesulfonic acid) (PIPES) and 99.999% KCl were purchased from Calbiochem. Phosphate-buffered saline (PBS) solution (10 mM Na_2HPO_4, 137 mM NaCl, 2.7 mM KCl, pH 7.4) was obtained from Corning Cellgro. Nitric oxide gas (Airgas) was purified by passing through an Ascarite (NaOH fused on silica gel) column and a 6 ft silica gel-filled coil cooled at −78 °C, and was collected in glass Schlenk storage bulbs which were subsequently sealed and stored under inert atmosphere in a glove box. Sodium α-oxyhyponitrite ($Na_2N_2O_3$, Angeli's salt) was prepared according to a previously published procedure.[8] *S*-nitroso-*N*-acetyl-DL-penicillamine (SNAP), *S*-nitrosoglutathione (GSNO), and sodium peroxynitrite (NaONOO) were purchased from Cayman Chemical. All other reagents for the spectroscopic studies were

purchased from Sigma-Aldrich. All spectroscopic measurements were conducted in aqueous buffer (50 mM PIPES, 100 mM KCl, pH 7.0), pretreated with Chelex resin (Bio-Rad) to remove residual metal ions in solution. The pH measurements were performed with a Mettler Toledo FE20 pH meter. Ultra-dry, high-purity 99.995% $CuCl_2$ (Alfa Aesar) was used to prepare 0.1 M volumetric solutions in deionized water and acetonitrile. $CuCl_2$ solutions of lower concentrations were prepared by dilution of 0.1 M volumetric solutions. Stock solutions of CLT/CuCLT (0.4, 1.3 or 2.0 mM in deionized water) and QLT/QLF (0.9 or 2.0 mM in spectroscopic grade DMSO) were stored at −40 °C in 50 μL aliquots, and thawed immediately before use. For all spectroscopic studies, stock solutions of the Cu(II) complexes of QLT and QLF were prepared in situ by combining a DMSO stock solution of the fluorescent ligand with 20 mM $CuCl_2$ aq in a 1:1 molar ratio, 30 min prior to the start of the measurements. All measurements were conducted at 25.0 or 37.0 °C, maintained by a circulating water bath. Extinction coefficients (ε) and fluorescence quantum yields (Φ) were determined in the 0.1−5 μM range in aqueous buffer solutions at pH 7.0. In determining the fluorescence quantum yields of metal-free and Cu(II)-bound CLT and QLT, excitation was provided at 550 nm, the emission spectra were integrated from 560 to 700 nm, and the calculations were standardized to resorufin (λ_{em} = 585 nm, λ_{ex} = 571 nm, and Φ = 0.74 at pH = 9.5[9]). In determining the fluorescence quantum yields of metal-free and Cu(II)-bound QLF, excitation was provided at 505 nm, the emission spectra were integrated from 510 to 650 nm, and the calculations were standardized to fluorescein (λ_{em} = 521 nm, λ_{ex} = 490 nm, and Φ = 0.95 in 0.1 M aq NaOH[10]). All measurements were repeated in triplicate.

Analyte Selectivity Studies. The analyte selectivity profiles of CuCLT, CuQLT, and CuQLF were determined by comparing the fluorescence emission spectra of 2 μM solutions of the sensors in aqueous buffer at pH 7.0, before and after treatment with 500 equiv of aq $ZnSO_4$, $NaNO_2$, KNO_3, NaClO, H_2O_2, NaONOO, sodium L-ascorbate, sodium glutamate, Na_2S, L-cysteine, glutathione, L-methionine, SNAP, GSNO, and Angeli's salt. Selectivity towards HO^- was studied in aq 10 mM NaOH. Stock solutions of Angeli's salt in aq 10 mM NaOH, GSNO in PBS buffer, and SNAP in aq 10 mM HCl were prepared anaerobically (O_2 < 1 ppm) under nitrogen atmosphere in a glove box dedicated to work with aqueous solutions ("wet box"), and brought out of the wet box in gastight syringes. For the NO, HNO, SNAP, GSNO, and peroxynitrite selectivity studies, the samples were prepared anaerobically in the wet box and

brought out in sealed airtight quartz cuvettes. NO gas, 1500 equiv, was removed from the side arm of a storage bulb inside the wet box with a gastight syringe and injected into the headspace of each airtight cuvette before measuring the fluorescence response. The selectivity studies for SNAP and GSNO were also performed aerobically. In addition, the reactivity of CuCLT and CuQLT toward H_2S was studied by bubbling H_2S gas, generated *in situ* from 6 M aq HCl and solid FeS, for 2 min through the aqueous solutions of the sensors. In each case, the integrated fluorescence emission spectrum recorded 20 min after addition of the analyte was normalized with respect to the integrated initial spectrum, arbitrarily assigned as unity. All measurements were repeated in triplicate. The detection limit (DL) of CuCLT and CuQLT for Angeli's salt and L-cysteine, respectively, was calculated according to the following equation:

$$\mathrm{DL} = (3 \times \sigma) / k$$

where σ is the standard deviation of the samples without analyte added, and k is the slope of the linear fit through the first 6 data points of the graphs of Figure 3, inset and Figure 4, respectively.

Apparent Cu(II) Dissociation Constants. The apparent Cu(II) dissociation constants (K_d) for the binding sites of QLT, QLF, and **S7** were determined by titration of aqueous 20 mM $CuCl_2$ into 2.0 mL of 5 μM (QLT, QLF) or 10 μM (**S7**) ligand solutions in aqueous buffer at pH 7.0 up to a final Cu^{2+} concentration of 50 μM. The formation of the Cu(II) complexes was monitored by the absorbance changes (ΔA) at 516, 492, and 259 nm, respectively (Figure S19). The absorbance change was plotted against the total Cu^{2+} concentration and fitted to the non-linear one-step binding equilibrium equation:[11]

$$\Delta A = \frac{\Delta A_\infty \times ([Cu^{2+}]_{total} + [L]_{total} + K_d - \sqrt{([Cu^{2+}]_{total} + [L]_{total} + K_d)^2 - 4 \times [L]_{total} \times [Cu^{2+}]_{total}})}{2 \times [L]_{total}}$$

where ΔA_∞ is the maximum absorbance change, $[L]_{total}$ is the total ligand concentration, and $[Cu^{2+}]_{total}$ is the total concentration of Cu^{2+} titrated in the solution. Under these conditions, the fit parameters obtained were: K_d = 3.3 ± 0.8, 15.0 ± 2.8, and 0.13 ± 0.03 μM, with R^2 = 0.9828, 0.9876, and 0.9992 for the QLT, QLF and **S7** ligands, respectively.

Cyclic Voltammetry. Cyclic voltammograms for metal-free and Cu(II)-bound CLT and QLT were measured using a three-electrode setup with a 2.0 mm diameter glassy carbon working electrode, a platinum auxiliary electrode, and a Ag/Ag^+ pseudoreference electrode in acetonitrile. The solvent contained 0.1 M *n*-Bu_4NPF_6 as the supporting electrolyte. The measurements were

performed at ambient temperature with a VersaSTAT3 potentiostat (Princeton Applied Research) operated with the V3 studio software, and were carried out at scan rates of 50 to 500 mV s^{-1} on quiescent solutions sparged with dry nitrogen for 5 min. Data in acetonitrile were referenced internally to the Fc/Fc^+ couple, added to the solution at the end of the measurements. In addition, the reduction potential of Cu(II) in CuCLT was measured in PBS aqueous buffer (pH 7.4) using a satd. Ag/AgCl in 3 M aq NaCl reference electrode ($E^0_{1/2}$ vs. NHE = 0.21 V).

Electron Paramagnetic Resonance (EPR) Spectroscopy. Low-temperature X-band EPR spectra (77 K, 9 GHz) were collected with a Bruker EMS spectrometer equipped with an ER 4199HS cavity and a Gunn diode microwave source. EPR samples were prepared anaerobically. Spectra were averaged over two sets of 10 scans. Solid CuCLT and QLT samples were brought into a glove box and dissolved in methanol to a final concentration of 400 μM. To prepare the CuQLT complex, 0.8 equiv of aqueous $CuCl_2$ were added to the QLT solution in methanol and kept for 30 min at ambient temperature. To monitor the reduction of Cu^{2+} in CuCLT, a solution of Angeli's salt (100 equiv) was prepared anaerobically in aq 10 mM NaOH and added to 350 μL of 400 μM CuCLT in methanol. To monitor the reduction of Cu^{2+} in CuQLT, a solution of L-cysteine (100 equiv) was prepared anaerobically in deionized water and added to 350 μL of 400 μM CuQLT in methanol. The samples were brought out of the glove box in sealed EPR tubes and immediately frozen in liquid nitrogen prior to acquisition of the EPR spectra. Spectra were simulated in Matlab using the solid-state/frozen-solution functionality ('pepper') implemented in EasySpin.[12]

Cell Culture and Staining Procedures. HeLa cells were cultured in Dulbecco's Modified Eagle Medium (DMEM, GIBCO), supplemented with 10% heat-deactivated fetal bovine serum (FBS) and 1% penicillin/streptomycin, at 37 °C in a humidified atmosphere with 5% CO_2. Cells were plated in 35 mm glass-bottom, poly-D-lysine coated culture dishes with 14 mm opening (MatTek) 24−48 h before imaging. All cells used were at a passage number from 5 to 15, and the experiments were repeated on cells from at least two separate frozen stocks at different passages. A confluence level of 40−60% was reached at imaging. Cells were incubated with the sensors and organelle stains at 37 °C for 15−20 min before mounting to the microscope. For all cell imaging studies, stock solutions of the Cu(II) complexes of QLT and QLF were prepared in situ by combining a DMSO stock solution of the fluorescent ligand with aq 20 mM $CuCl_2$ in a 1:1

molar ratio 30 min prior to incubation. Stock solutions of Cu_2FL2E were prepared in situ by combining a DMSO stock solution of the FL2E ligand with aq 20 mM $CuCl_2$ in a 1:2 molar ratio 20 min prior to incubation. The growth medium was replaced with 2 mL of fresh dye- and serum-free DMEM (for CuCLT) or PBS (for CuQLT), to which the sensor and selected organelle stains were added before incubation. The organelle-specific dyes employed in the colocalization experiments for CuCLT were: Hoechst 33258 (Invitrogen, final concentration 15 μM), MitoTracker Green (Invitrogen, final concentration 0.25−0.5 μM), ER-Tracker Green (Invitrogen, final concentration 1 μM), and LysoTracker Green (Invitrogen, final concentration 0.1 μM). In order to block intracellular free thiols, cells were pre-incubated with *N*-methylmaleimide (TCI, final concentration 1 mM) in PBS buffer for 30 min, followed by rinsing with 2 mL of PBS prior to sensor incubation. To increase the intracellular nitrosothiol content, cells were incubated with DETA NONOate (Cayman Chemical, final concentration 200 μM) for 20 h in DMEM, followed by rinsing with 2 mL of PBS prior to sensor incubation. Cells were rinsed with sterile PBS buffer (2 × 2 mL) to remove excess unbound dyes. For all imaging experiments, cells were bathed in 2 mL of PBS buffer (pH = 7.4) before mounting on the microscope stage. After the initial sets of images were acquired, intracellular fluorescence changes were measured following addition to the PBS buffer of concentrated aqueous stock solutions of selected analytes (Angeli's salt, Na_2S, GSNO, L-cysteine, or sodium L-ascorbate) to reach a final concentration of 1.25−1.5 mM in the imaging dish.

Cytotoxicity of CuCLT. The cytotoxicity of CuCLT was evaluated by the MTT assay. A stock solution of the sensor was freshly prepared in deionized water before use. HeLa cells were plated in a 96-well plate (~4000 cells per well) in 100 μL of DMEM and incubated for 24 h. The cells were then treated with 100 μL of 1 to 5 μM DMEM solutions of CuCLT for an incubation period of 24 h at 37 °C, the medium containing the sensor was removed and replaced with 200 μL of a solution of 3-(4,5-dimethylthiazol-2-yl)-2,5-diphenyltetrazolium bromide (MTT) (1 mg/mL in PBS/DMEM = 1:4 v/v), and the cells were further incubated for 4 h. After removal of the medium, 200 μL of DMSO was added to each well to dissolve the violet crystals, and then the absorbance of the purple formazan dye was recorded at 570 nm using a BioTek Synergy HT multi-detection microplate reader. The reported percentage of cell survival values was normalized to control cells from the same plate with no probe added.

Fluorescence Microscopy. Fluorescence imaging experiments were carried out on a Zeiss Axiovert 200M inverted epifluorescence microscope equipped with a Hamamatsu EM-CCD C9100 digital camera and an MS200 XY Piezo Z stage (Applied Scientific Instruments). An XCite 120 metal halide lamp (EXFO) was used as the light source. Zeiss standard filter sets 49, 38 HE, and 43 HE were employed for acquiring images in the blue, green, and white channels, respectively. The microscope was operated with the aid of the Volocity software (version 6.01, Improvision). The acquisition of images of a given culture dish was performed at constant exposure time and sensitivity for each channel. The ImageJ software (version 1.47, NIH) was employed for quantification of intracellular fluorescence intensity. For each measurement, the whole cell was selected as region of interest and the integrated fluorescence from the background region was subtracted from the integrated fluorescence intensity of the cell body region. In order to evaluate co-localization of the sensors with organelle-specific stains, Pearson's correlation coefficients were calculated for individual cells with the PSC Colocalization plugin of ImageJ, choosing in each case the maximum background fluorescence signal as threshold. The images employed in co-localization studies were deconvoluted using Volocity iterative restoration algorithms.

Table S1. Photophysical parameters of CLT, QLT and QLF in aqueous buffer, pH = 7.0

	Metal-free					**Cu^{2+}-bound**				
	absorption		emission			absorption		emission		
probe	λ_{max} (nm)	$\varepsilon \times 10^{-4}$ (M^{-1} cm^{-1})	λ_{ex} (nm)	λ_{max} (nm)	Φ (%)	λ_{max} (nm)	$\varepsilon \times 10^{-4}$ (M^{-1} cm^{-1})	λ_{ex} (nm)	λ_{max} (nm)	Φ (%)
CLT	552	5.56 ± 0.14	550	580	66.8 ± 3.0	552	6.60 ± 0.05	550	579	11.9 ± 0.4
QLT	556	2.94 ± 0.06	550	580	18.4 ± 0.5	556	2.79 ± 0.04	550	580	12.9 ± 0.8
QLF	511	1.94 ± 0.02	505	531	12.0 ± 0.6	511	1.86 ± 0.01	505	530	9.0 ± 0.3

Scheme S6. Production of HNO from *S*-nitrosothiols (RSNO) and ascorbate[13]

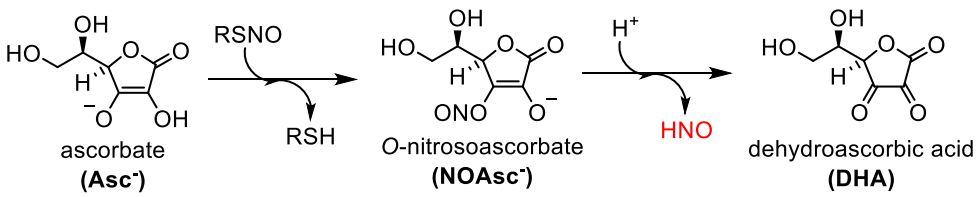

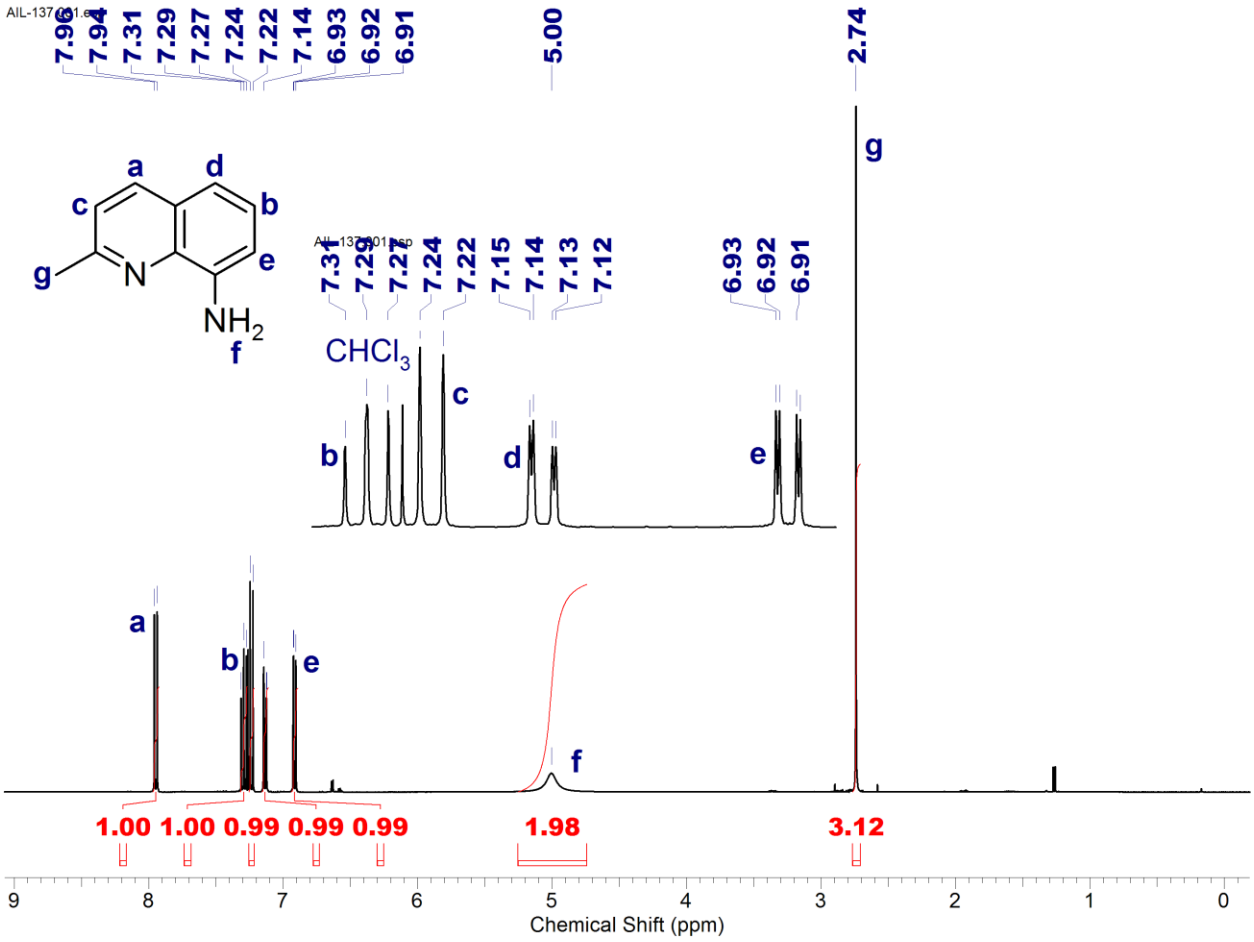

Figure S1. ^{1}H NMR spectrum of compound **S5** (400 MHz, $CDCl_3$).

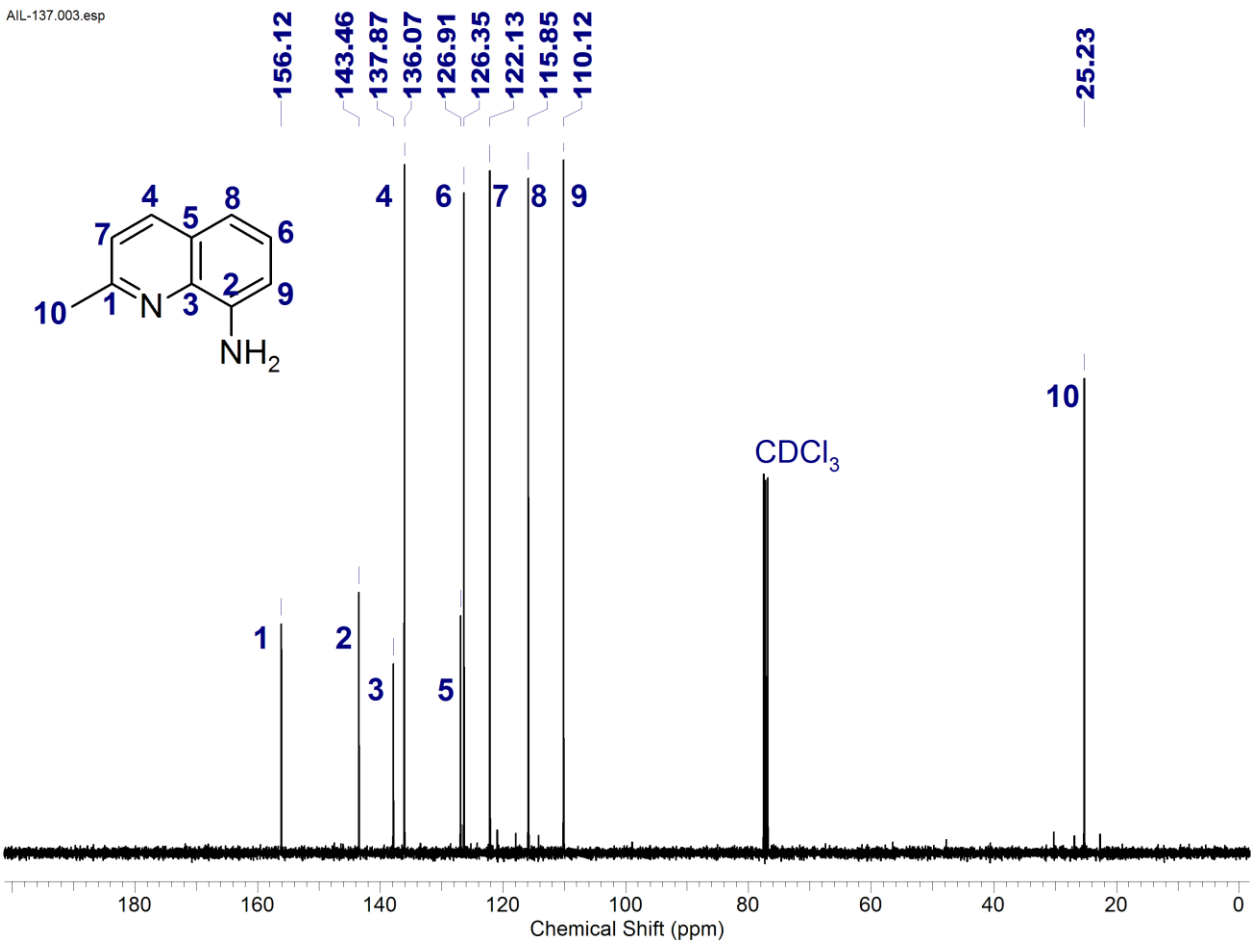

Figure S2. ^{13}C {^{1}H} NMR spectrum of compound **S5** (100 MHz, $CDCl_3$).

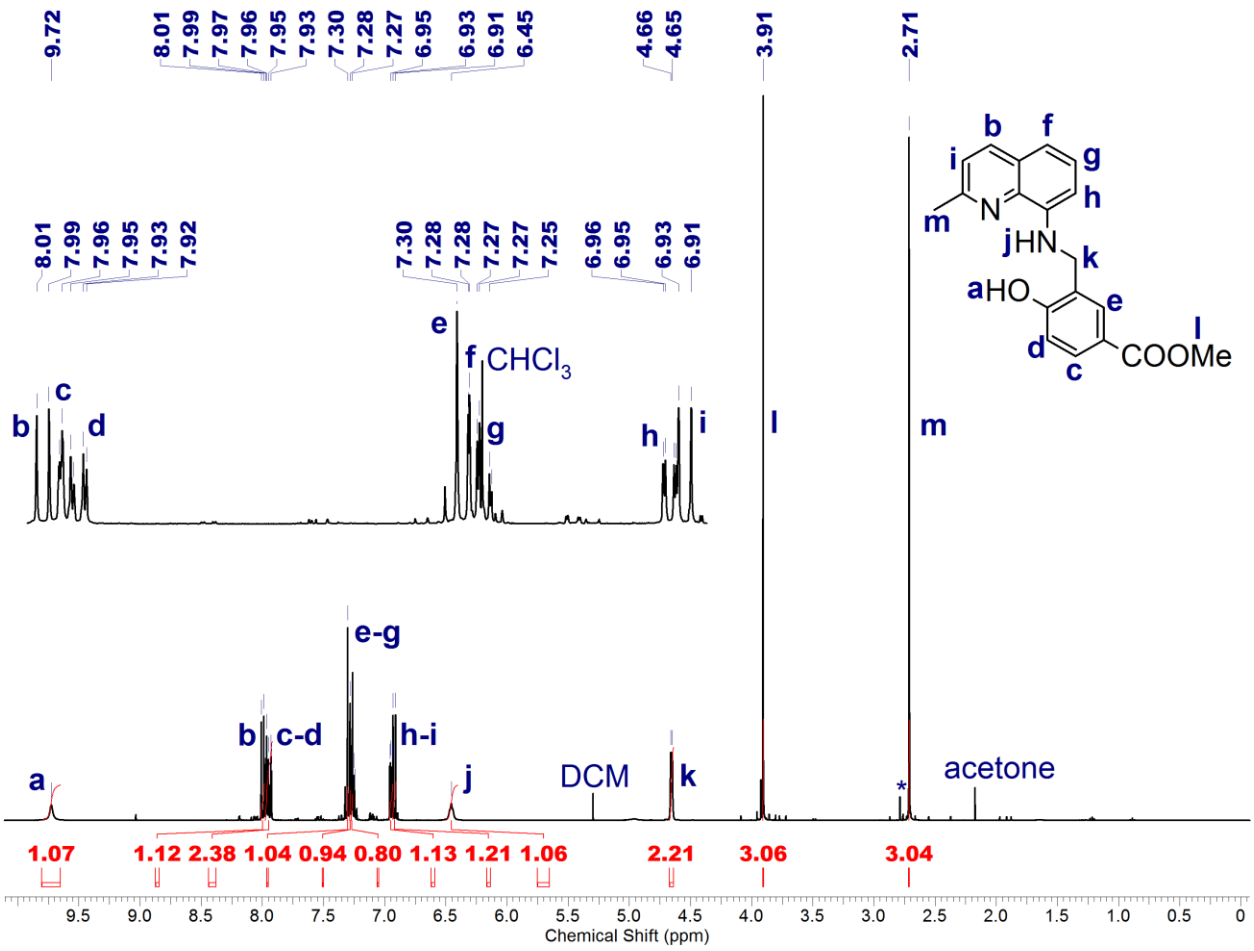

Figure S3. ^{1}H NMR spectrum of compound **S7** (400 MHz, $CDCl_3$).

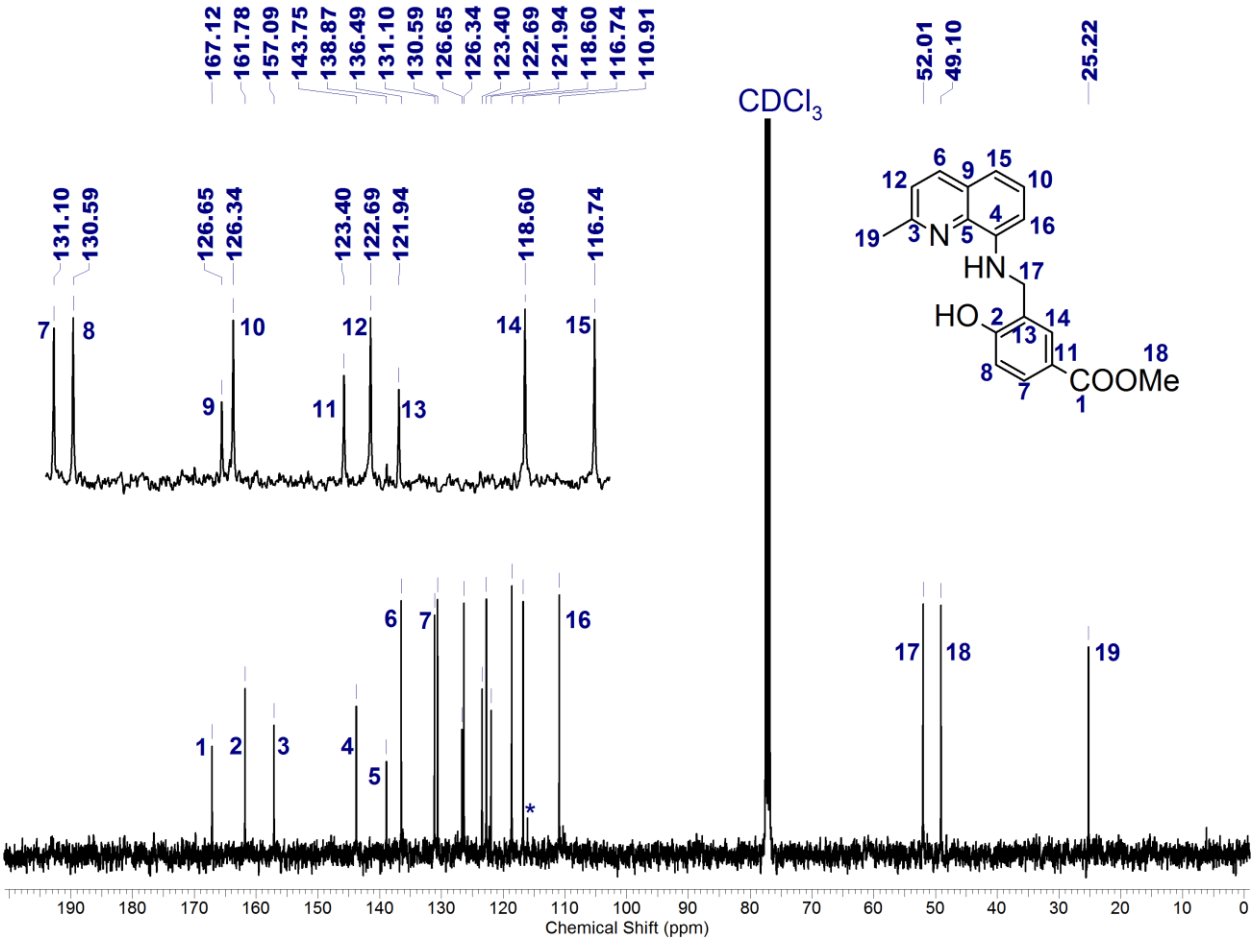

Figure S4. ^{13}C {^{1}H} NMR spectrum of compound **S7** (100 MHz, $CDCl_3$).

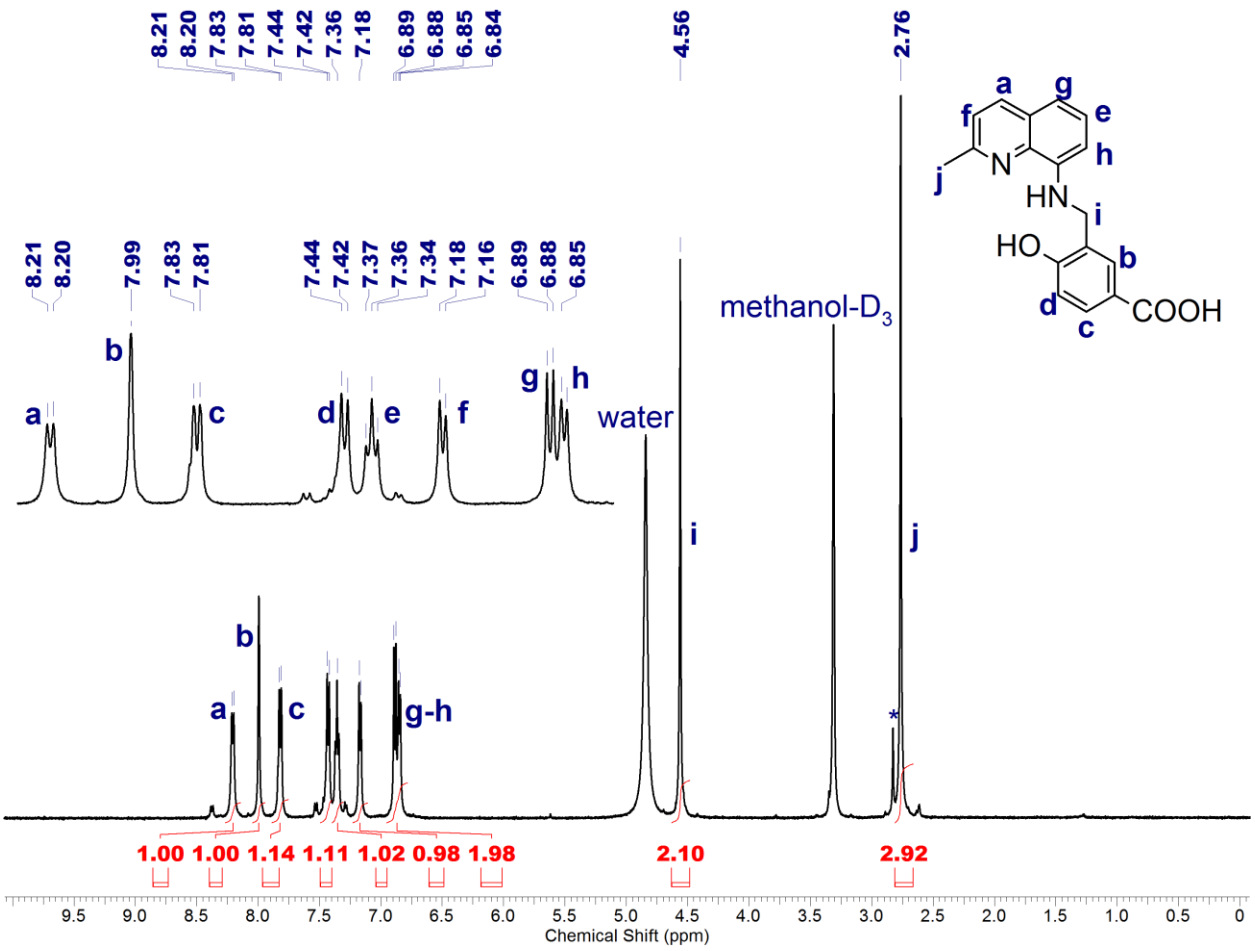

Figure S5. [1] H NMR spectrum of compound **S8** (500 MHz, $CD_3OD/CDCl_3$ = 4:1 with a drop of $(CD_3)_2SO$).

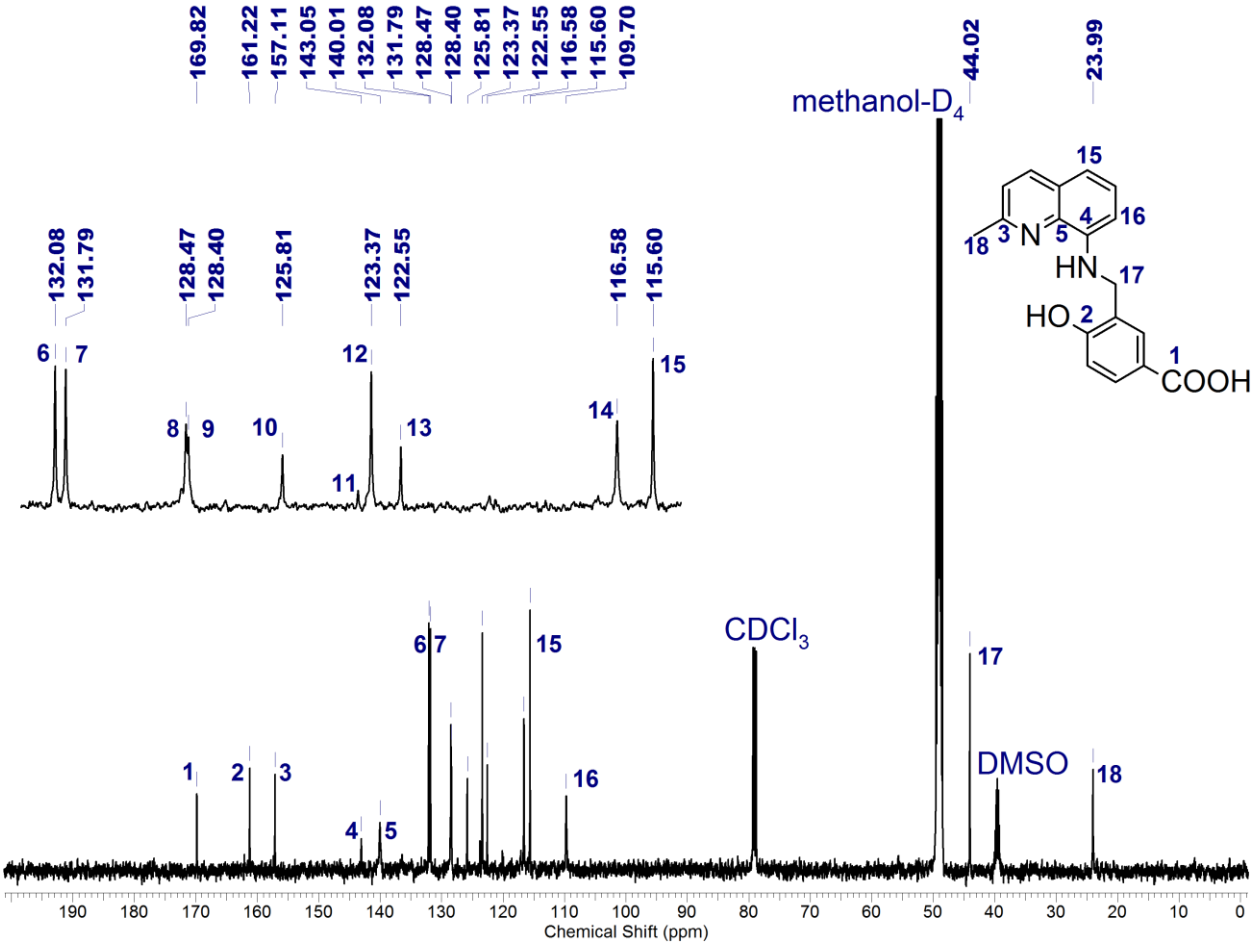

Figure S6. ^{13}C {^{1}H} NMR spectrum of compound **S8** (125 MHz, $CD_3OD/CDCl_3$ = 4:1 with a drop of $(CD_3)_2SO$).

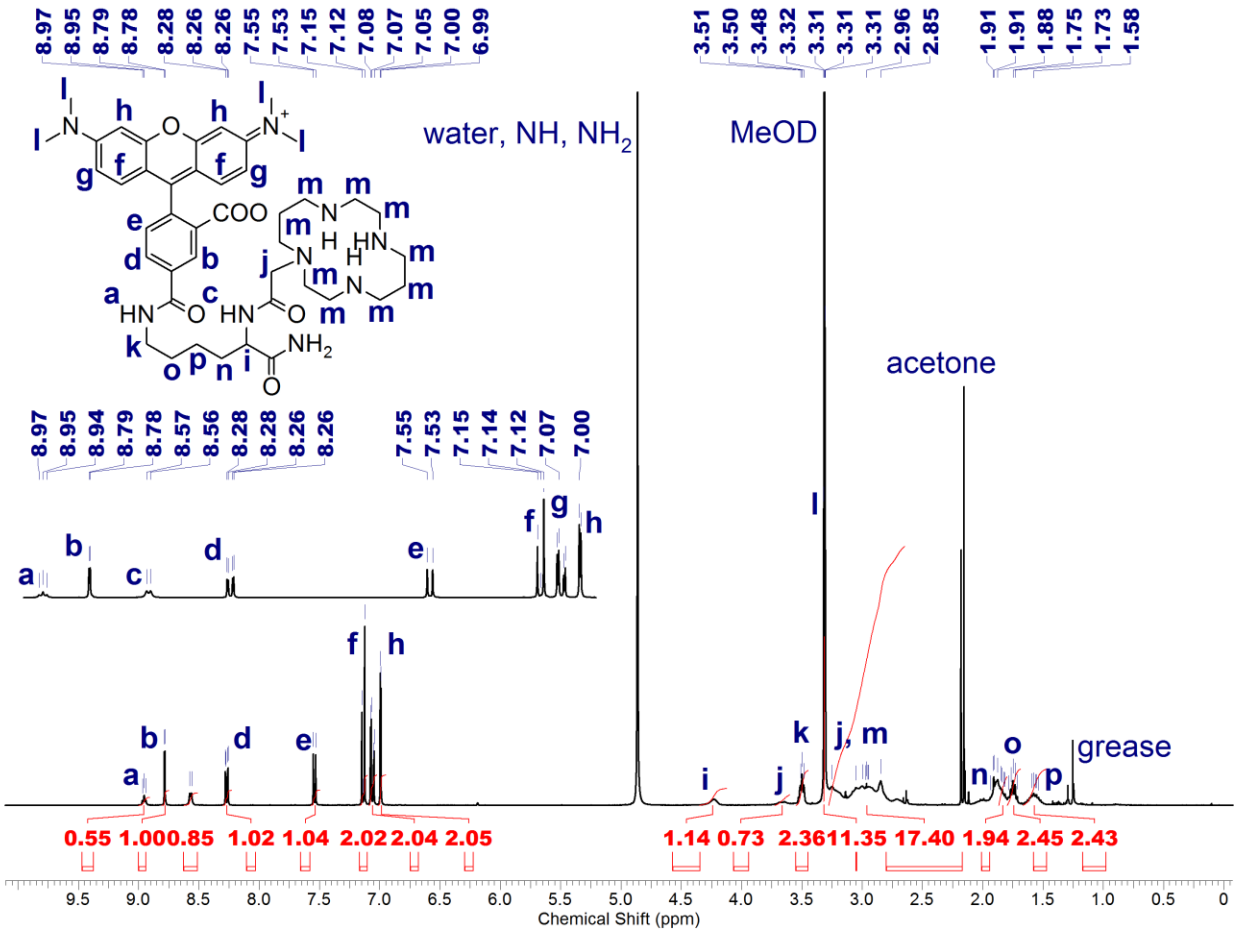

Figure S7. [1] H NMR spectrum of cyclam-Lys-TAMRA, CLT (400 MHz, CD_3OD).

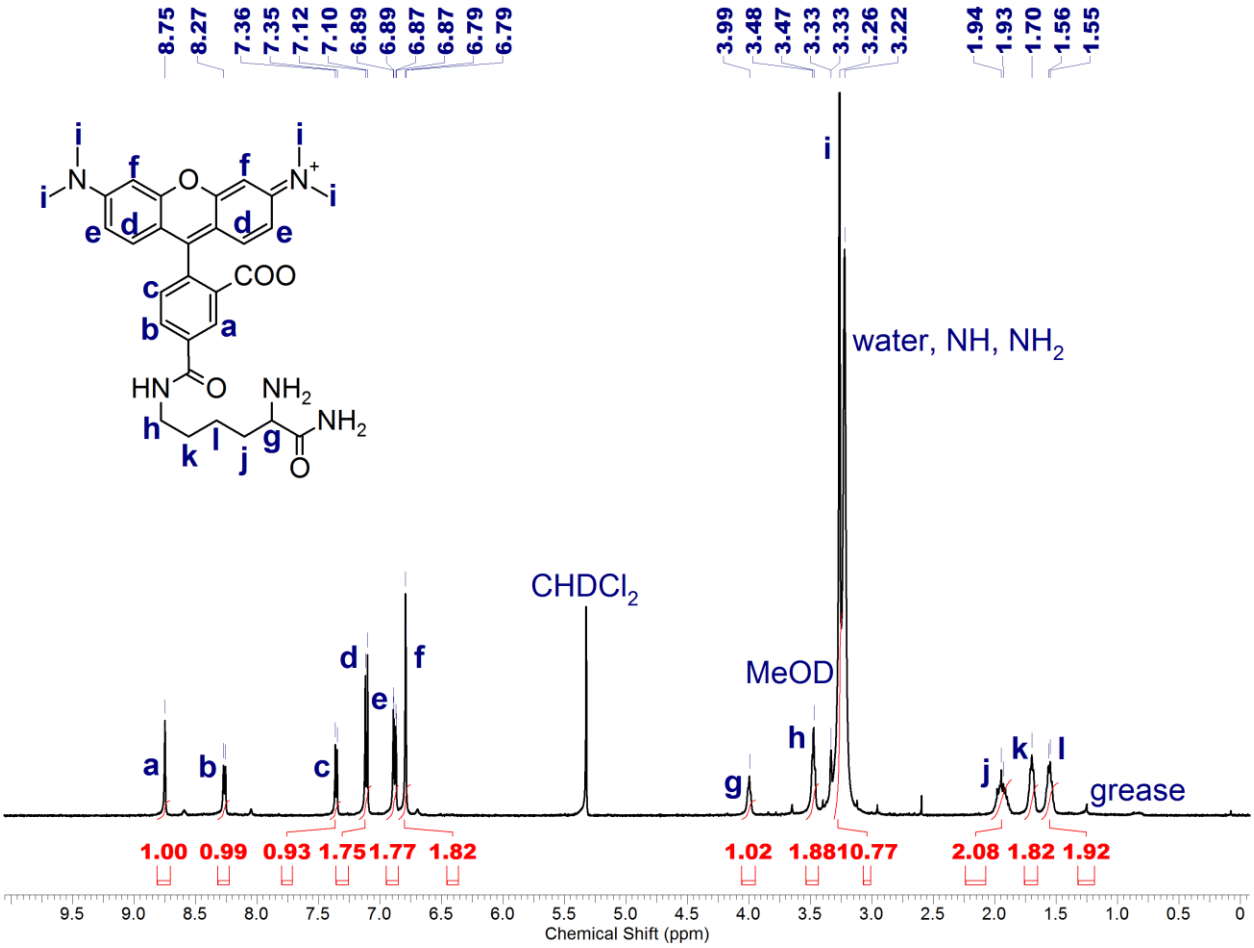

Figure S8. [1] H NMR spectrum of compound **S10**, H-Lys-TAMRA (500 MHz, CD_2Cl_2/CD_3OD = 9:1).

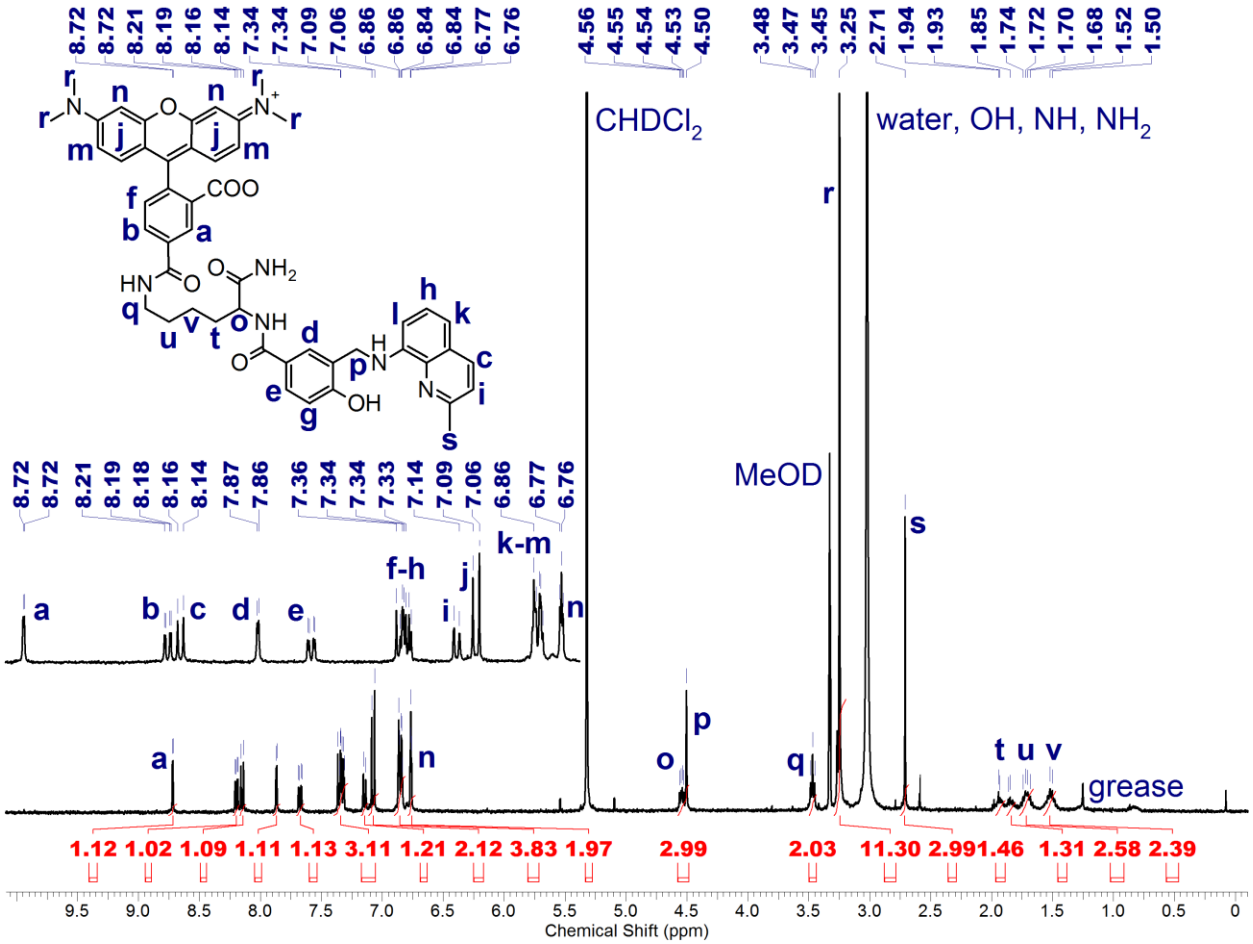

Figure S9. [1] H NMR spectrum of quin-Lys-TAMRA, QLT (400 MHz, CD_2Cl_2/CD_3OD = 9:1).

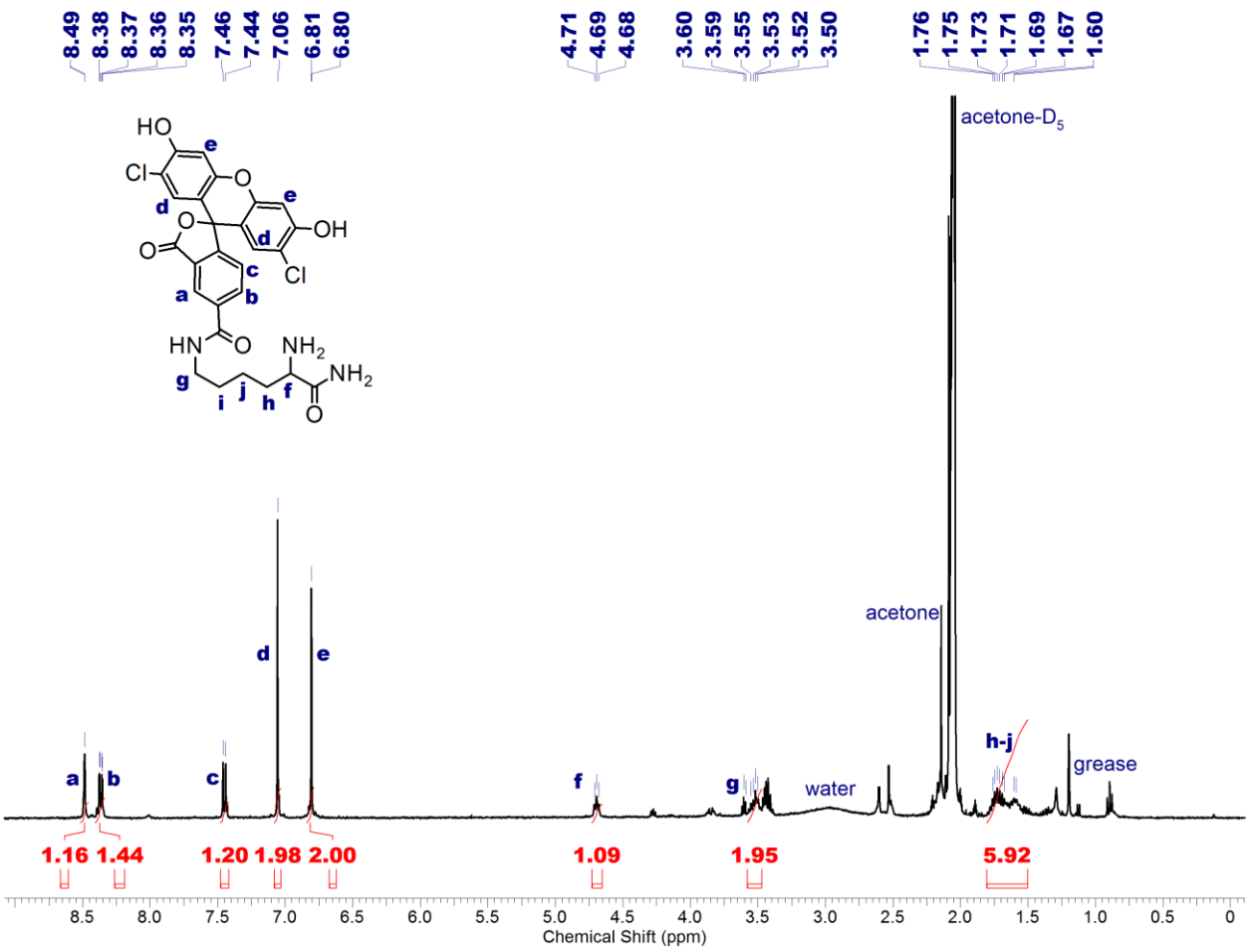

Figure S10. ^{1}H NMR spectrum of compound **S11**, H-Lys-fluorescein (400 MHz, $(CD_3)_2CO$).

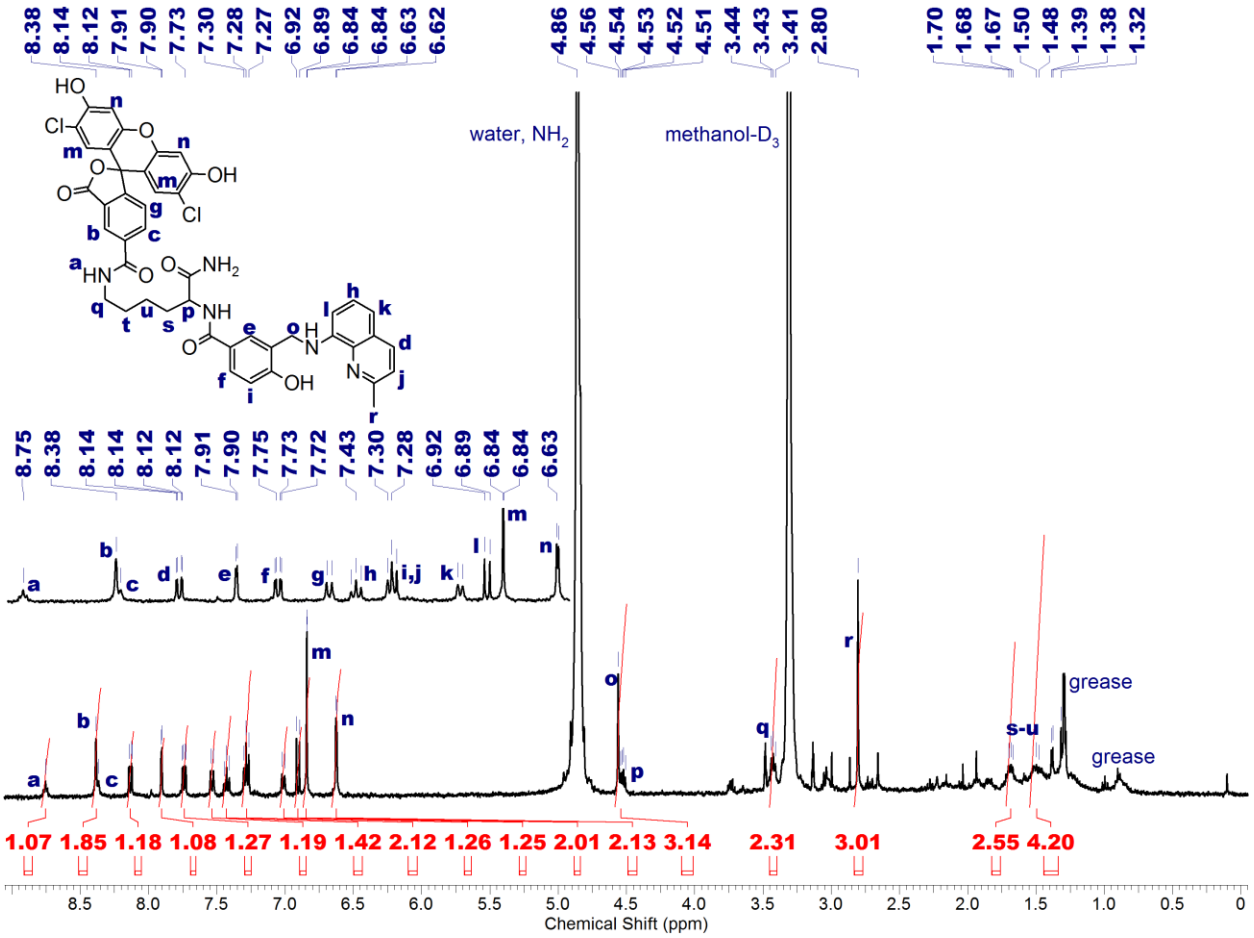

Figure S11. ^{1}H NMR spectrum of quin-Lys-fluorescein, QLF (400 MHz, CD_3OD).

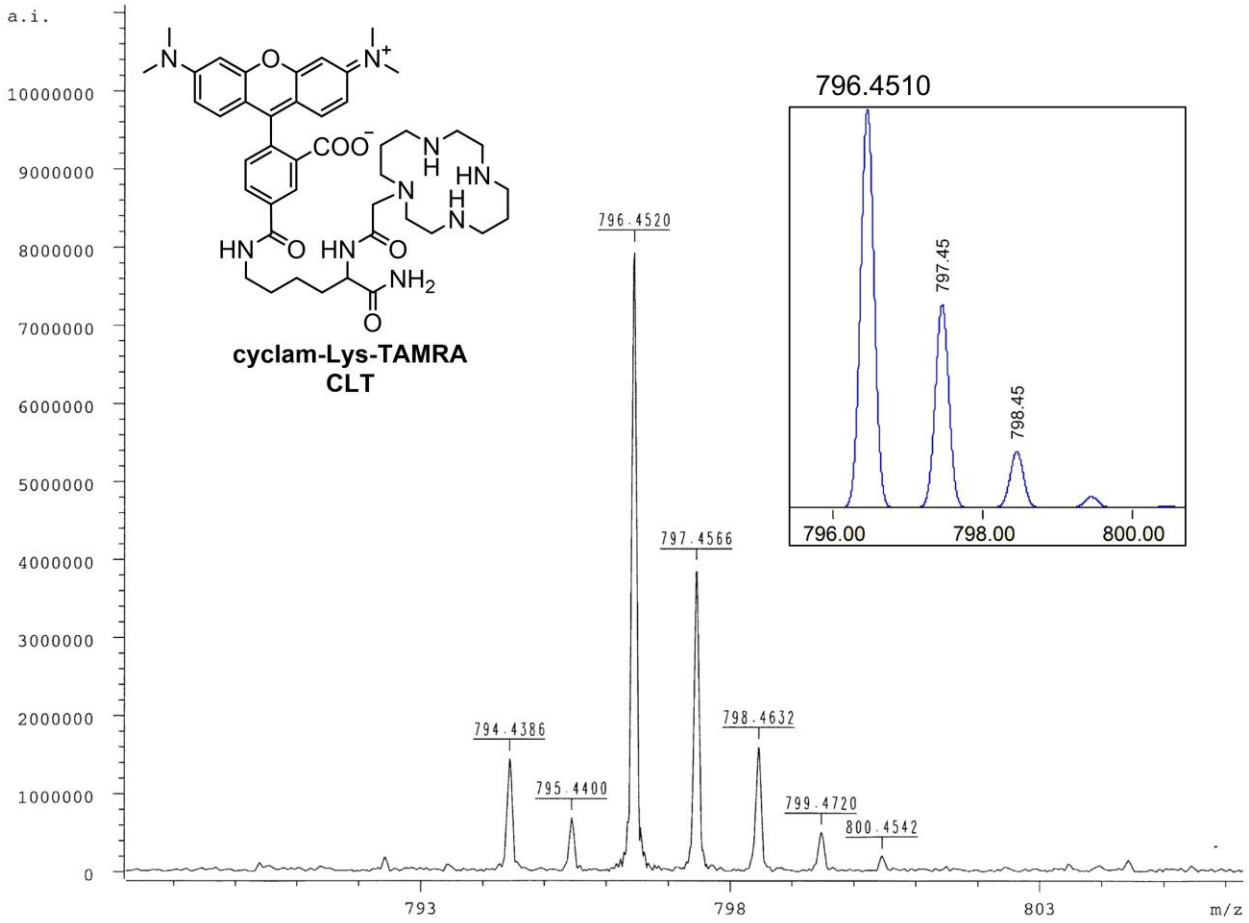

Figure S12. High-resolution mass spectrum (ESI−) of cyclam-Lys-TAMRA, CLT. Inset: calculated isotope pattern and exact mass.

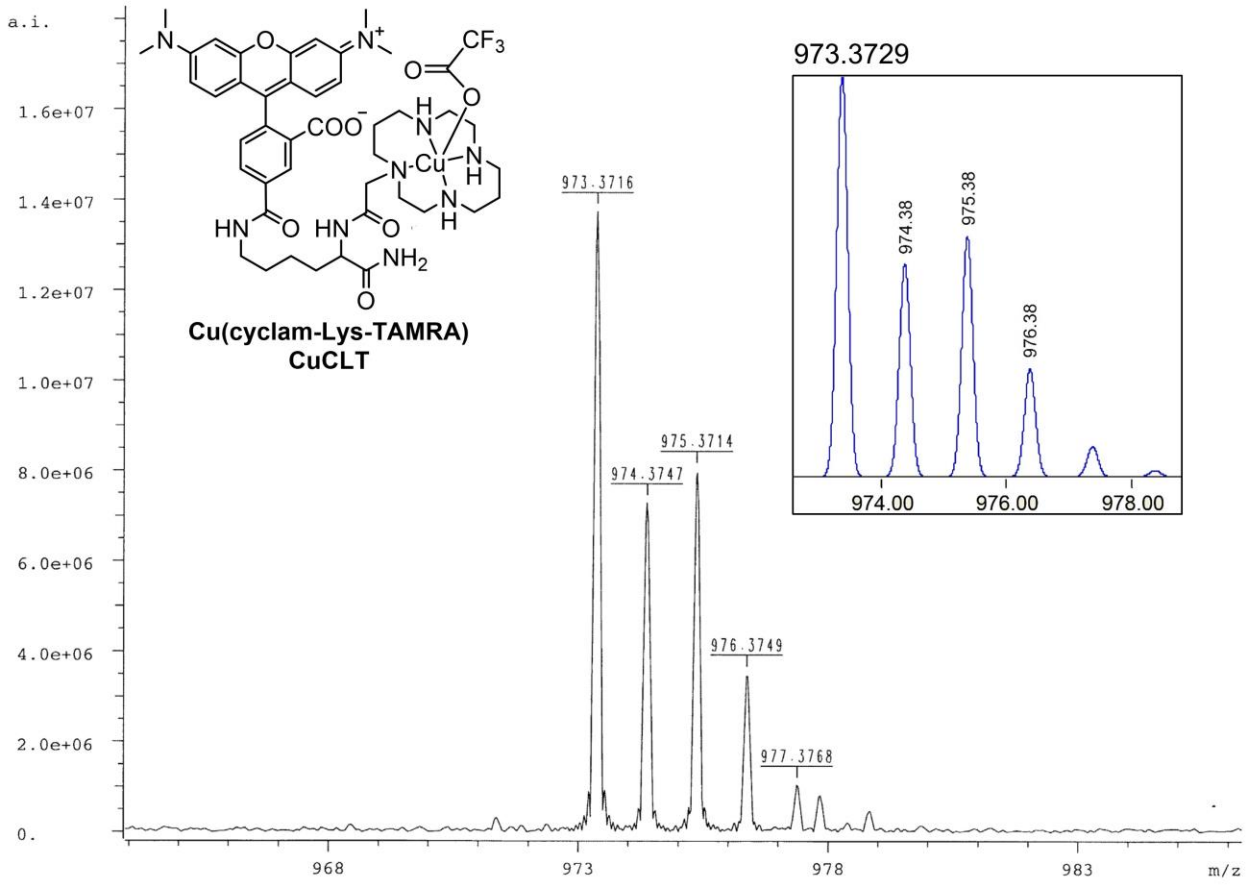

Figure S13. High-resolution mass spectrum (ESI+) of the TFA adduct of Cu(cyclam-Lys-TAMRA), CuCLT. Inset: calculated isotope pattern and exact mass.

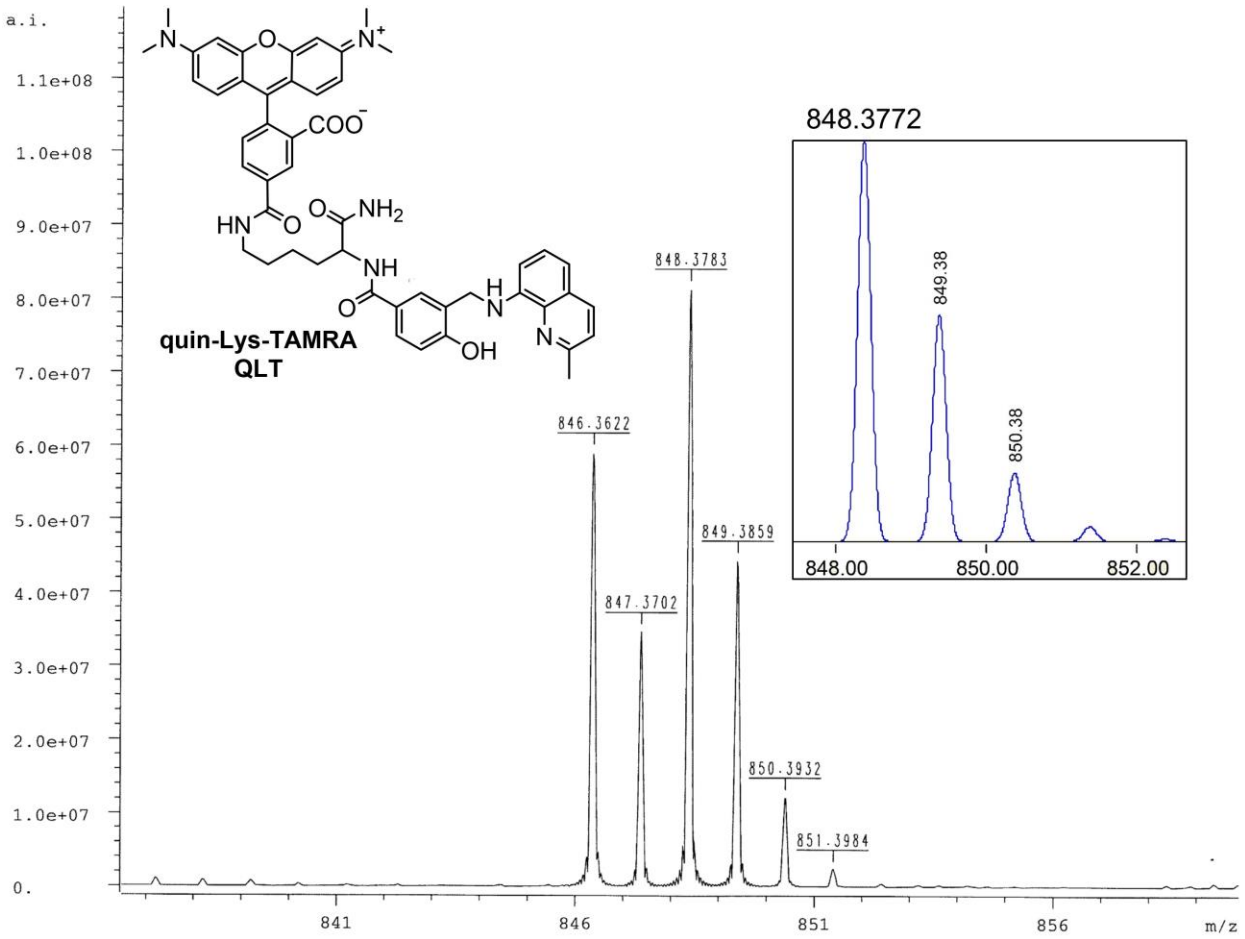

Figure S14. High-resolution mass spectrum (ESI+) of quin-Lys-TAMRA, QLT. Inset: calculated isotope pattern and exact mass.

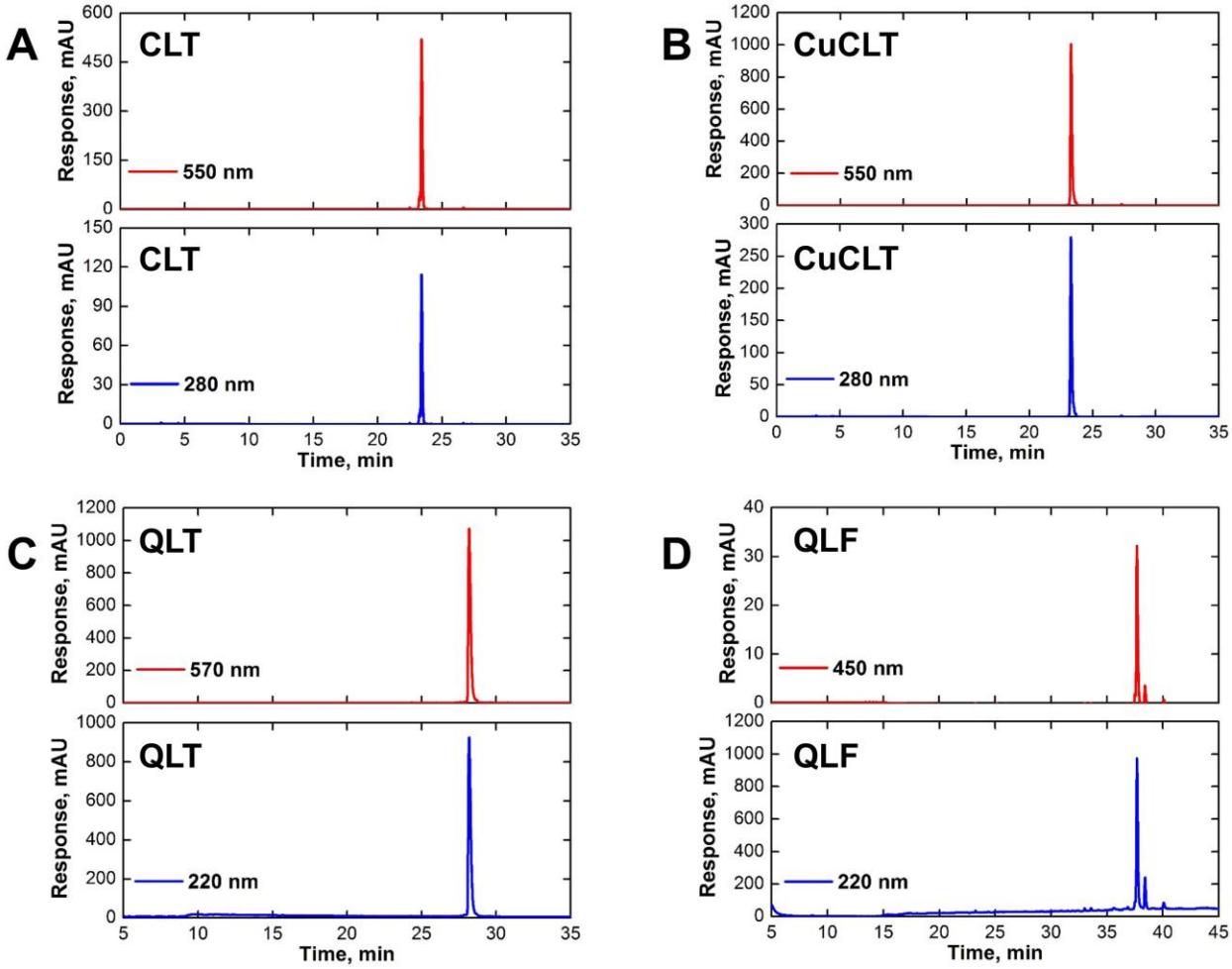

Figure S15. Analytical HPLC traces of (A) cyclam-Lys-TAMRA (CLT), (B) Cu(cyclam-Lys-TAMRA) (CuCLT), (C) quin-Lys-TAMRA (QLT), and (D) quin-Lys-fluorescein (QLF), detected by the signals at indicated wavelengths.

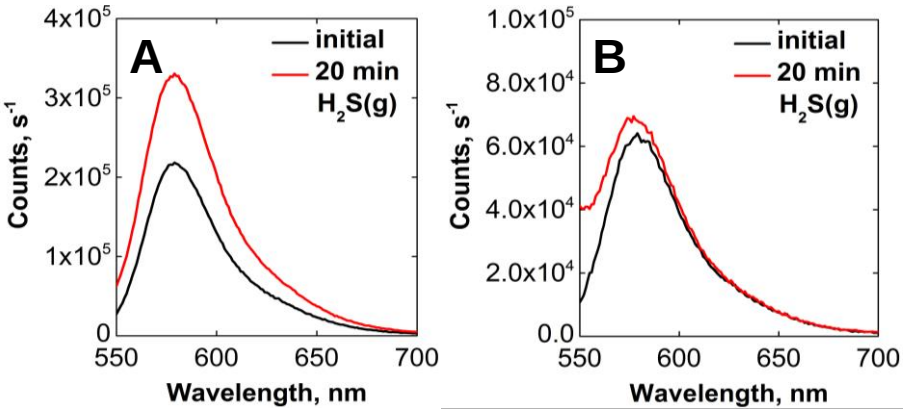

Figure S16. Fluorescence emission spectra of 2 μM of (A) CuCLT and (B) CuQLT, recorded before and 20 min after saturating the aqueous solutions by H_2S gas for 2 min (25 °C, 100 mM KCl, 50 mM PIPES, λ_{ex} = 540 nm).

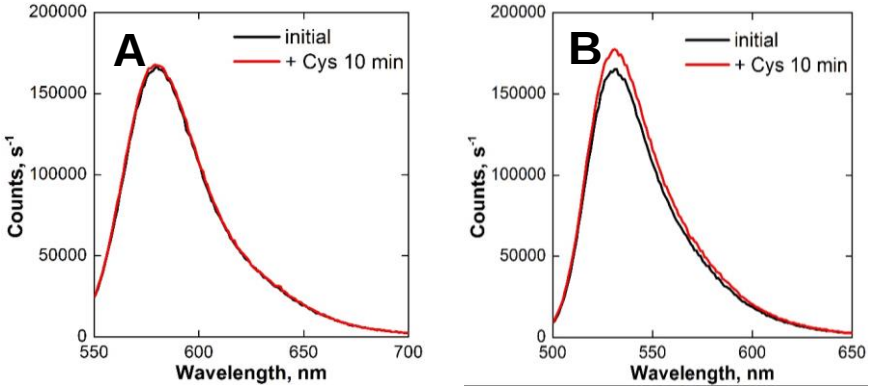

Figure S17. Fluorescence emission spectra of 2.5 μM solutions of (A) QLT and (B) QLF in aqueous buffer, recorded before and 10 min after addition of 500 equiv of L-cysteine (37 °C, 100 mM KCl, 50 mM PIPES, pH 7.0, λ_{ex} = 540 nm).

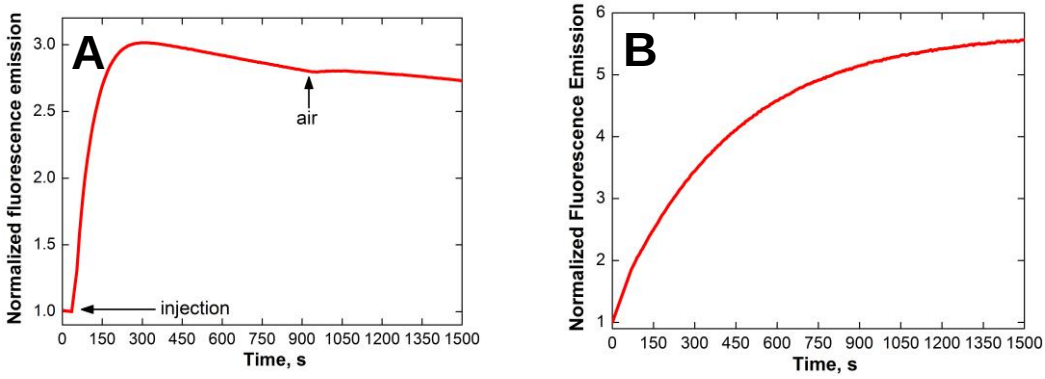

Figure S18. Plots of normalized fluorescence emission at 580 nm over time of (A) anaerobic 5 μM CuCLT and (B) 5 μM CuQLT solutions in aqueous buffer (25 °C, 100 mM KCl, 50 mM PIPES, pH 7.0, λ_{ex} = 540 nm), upon addition of 500 equiv of Angeli's salt and L-cysteine, respectively. The arrows in (A) indicate the points of injection of the analyte solution and exposure of the anaerobic mixture to air, respectively.

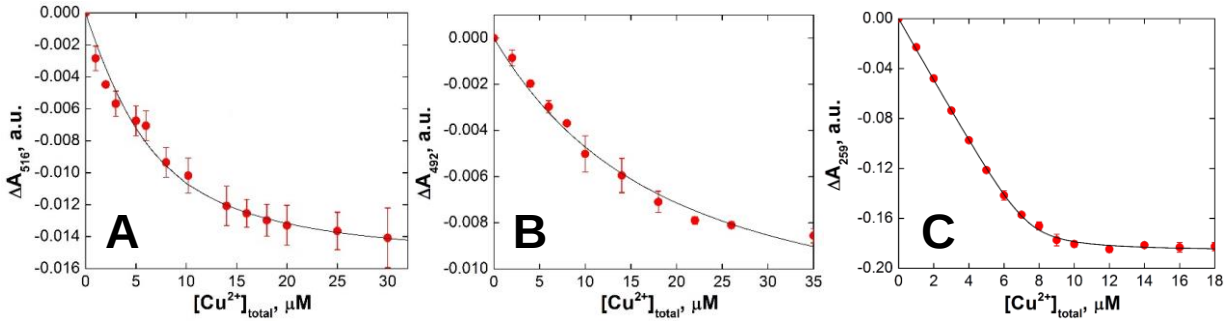

Figure S19. Determination of the dissociation constant (K_d) of (A) CuQLT, (B) CuQLF, and (C) **Cu-S7**. $CuCl_2$ was titrated into 5 μM solutions of QLT or QLF, or 10 μM solutions of **S7** in aqueous buffer (25 °C, 100 mM KCl, 50 mM PIPES, pH 7.0). The formation of the Cu(II) complexes of QLT, QLF and **S7** was monitored by the absorbance changes (ΔA) at 516, 492 and 259 nm, respectively. The titration traces were fit to a one step binding equation.

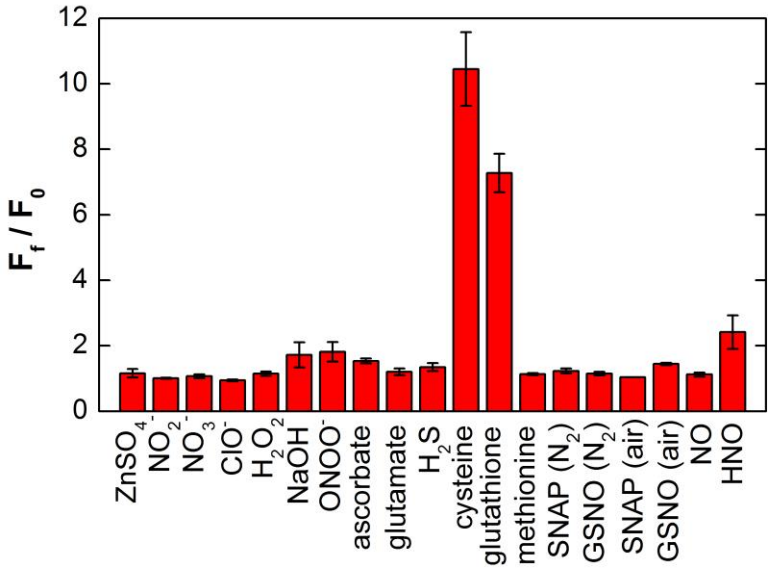

Figure S20. Selectivity of 2 μM CuQLF toward reactive nitrogen and oxygen species and other biological analytes in aqueous buffer (37 °C, 100 mM KCl, 50 mM PIPES, pH 7.0). For each sample, the fluorescence emission was recorded before and 20 min after addition of excess analyte (1500 equiv NO, 500 equiv all other). The measurements for OH^- were conducted in 10 mM aq NaOH. The integrated fluorescence intensity was normalized in each case to the initial value of the metal-bound complex. Excitation was provided at 490 nm, and fluorescence emission was integrated between 500 and 650 nm.

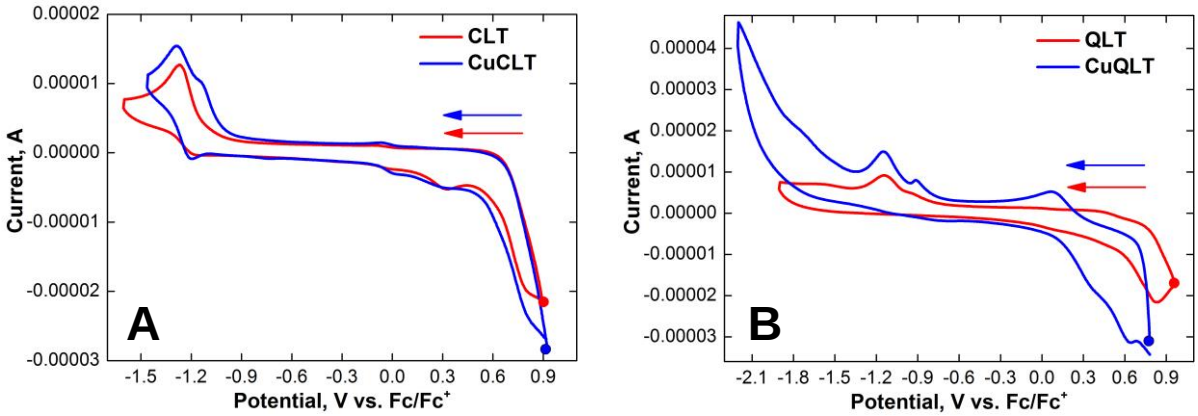

Figure S21. Cyclic voltammograms of 1 mM solutions of (red) metal-free and (blue) Cu(II)-bound (A) CLT and (B) QLT in acetonitrile containing 0.1 M *n*-Bu_4NPF_6 as the supporting electrolyte, using a glassy carbon working electrode, Pt auxiliary electrode, and Ag pseudo reference electrode. The potentials are referenced to the Fc/Fc^+ internal standard, added to the solution at the end of the measurements. Scan rate = 200 mV/s.

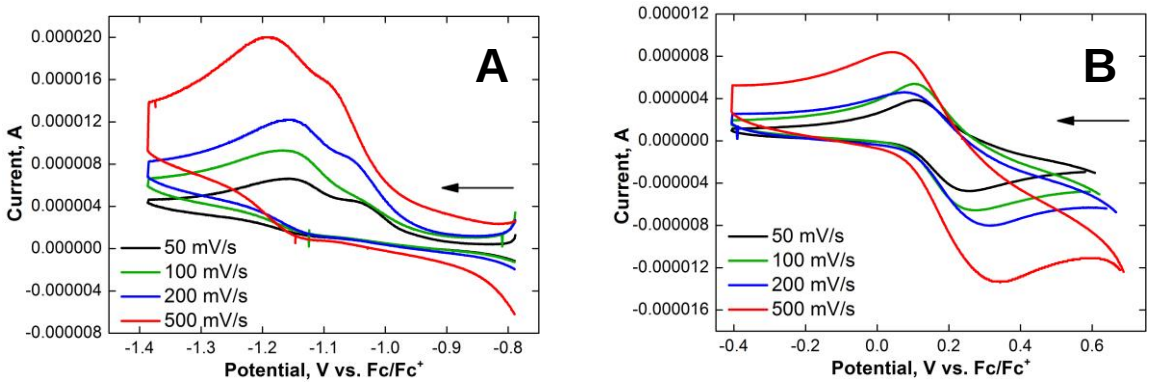

Figure S22. Cyclic voltammograms showing the Cu(II)-centered reduction of 1 mM solutions of (A) CuCLT and (B) CuQLT, measured at gradually increasing scan rates in acetonitrile containing 0.1 M *n*-Bu_4NPF_6 as the supporting electrolyte. The potentials are referenced to the Fc/Fc^+ internal standard.

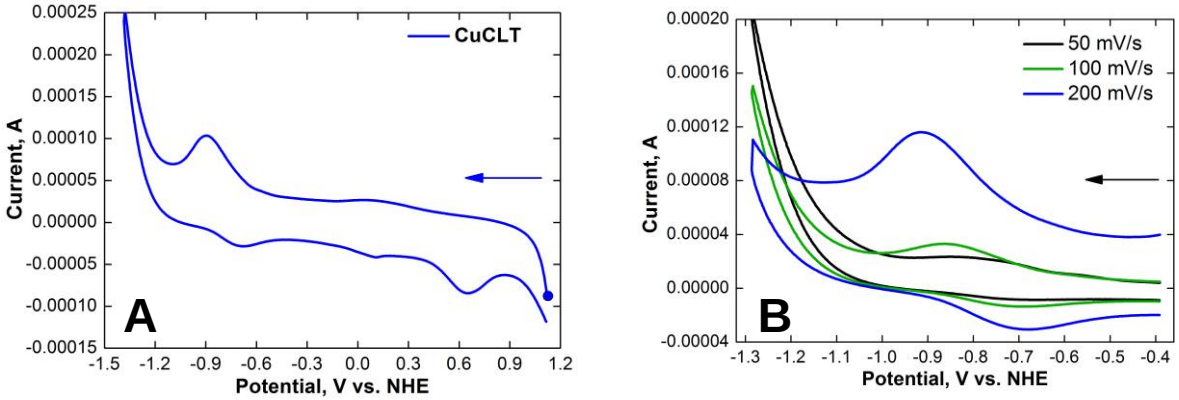

Figure S23. Cyclic voltammograms of 1 mM CuCLT in PBS aqueous buffer, using a glassy carbon working electrode, Pt auxiliary electrode, and satd. Ag/AgCl in 3 M aq NaCl reference electrode ($E^0_{1/2}$ vs. NHE = 0.21 V). (A) Wide range scan at 200 mV/s. (B) Quasi-reversible reduction of Cu(II) measured at various scan rates.

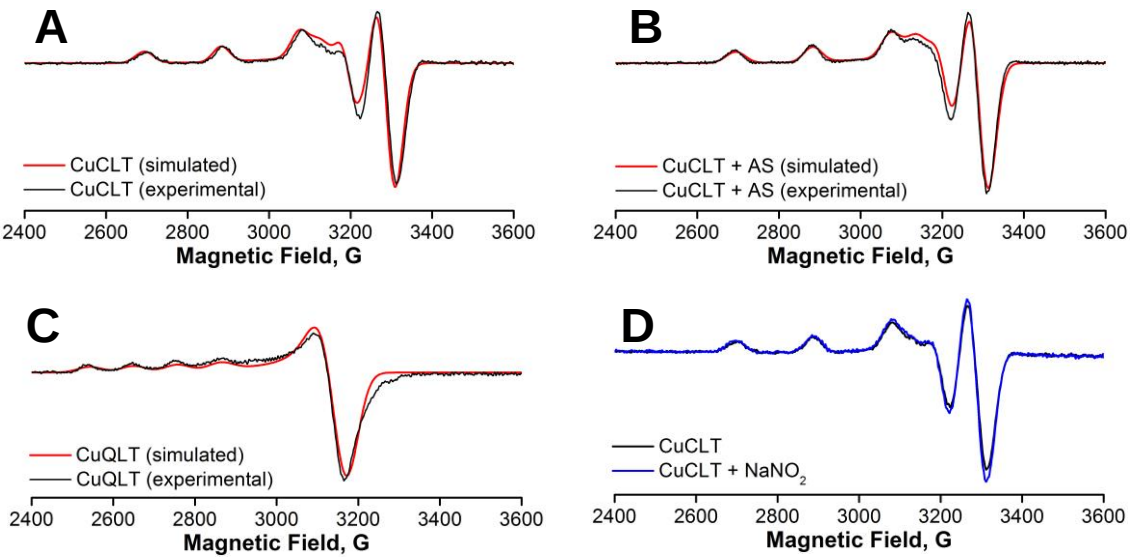

Figure S24. EPR spectra of CuCLT and CuQLT in methanol at 77 K. (A-C) Overlay of experimental (black) and simulated (red) spectra of 400 μM of (A) CuCLT, (B) CuCLT + 100 equiv Angeli's salt (AS), and (C) CuQLT. (D) EPR spectra of 400 μM solutions of CuCLT recorded in the absence (black) and after the addition (blue) of 100 equiv of $NaNO_2$.

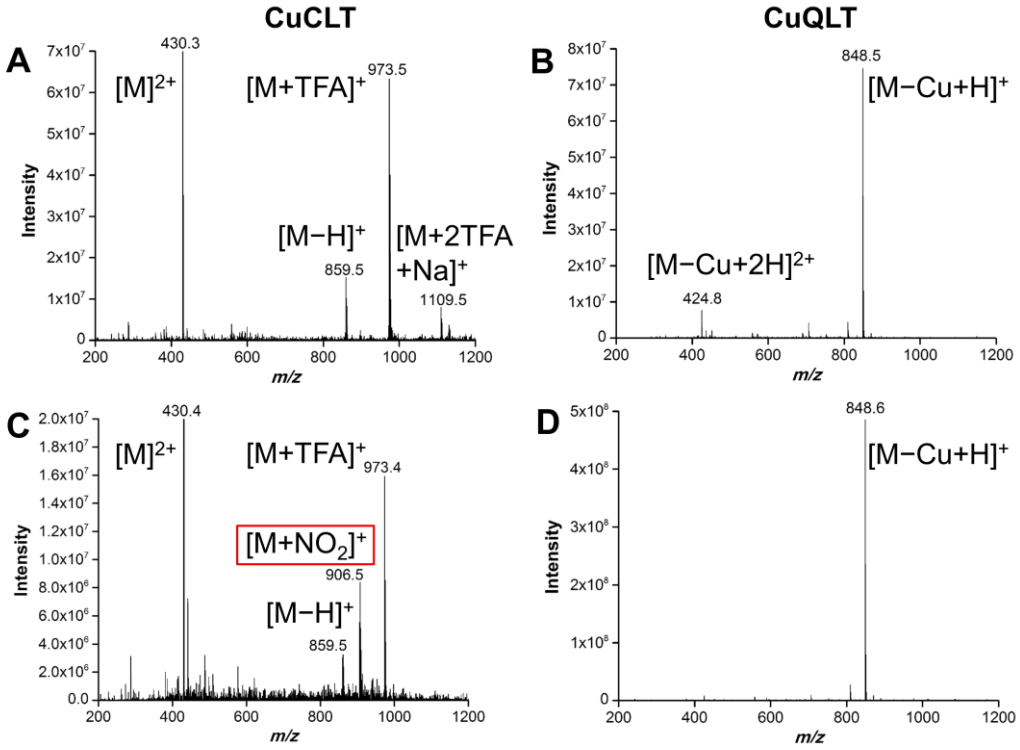

Figure S25. Low-resolution mass spectra (ESI+) of the 400 μM solutions of CuCLT and CuQLT in methanol used in the EPR spectroscopic studies and the assignment of observed peaks. Left: CuCLT (A) in the absence, and (C) with 100 equiv of Angeli's salt. Right: CuQLT (B) in the absence and (D) with 100 equiv of L-cysteine.

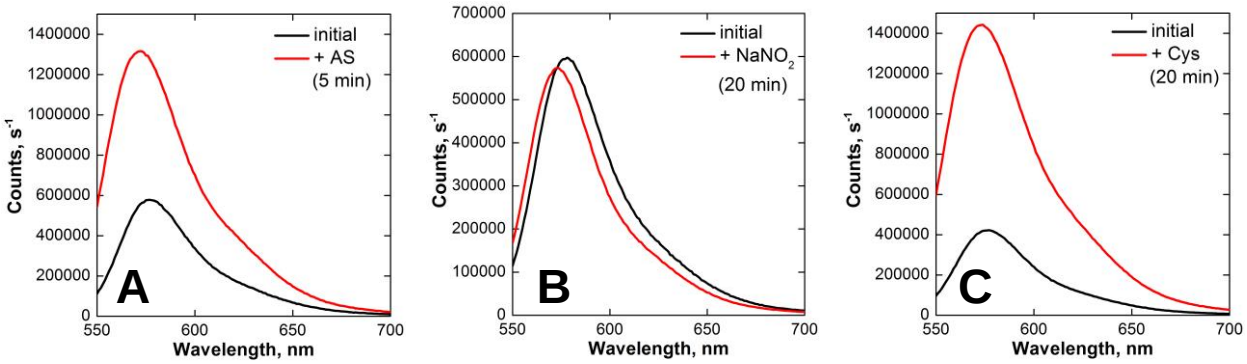

Figure S26. Fluorescence emission spectra of 5 µM anaerobic solutions of (A, B) CuCLT and (C) CuQLT in methanol, recorded before and after addition of 100 equiv of Angeli's salt, $NaNO_2$, and L-cysteine, respectively (25 °C, λ_{ex} = 540 nm).

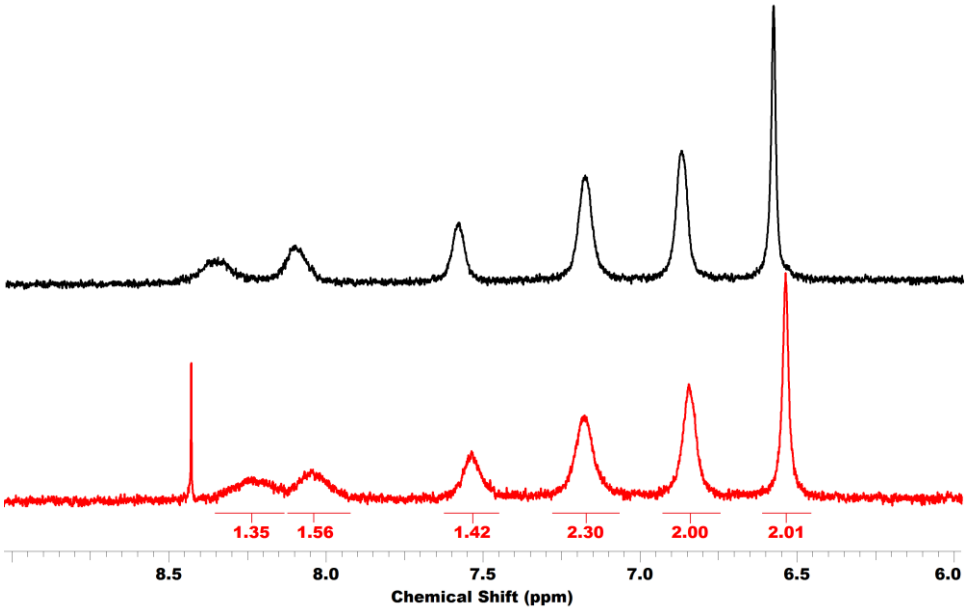

Figure S27. Aromatic region of the ^{1}H NMR spectra of a 3.5 mM anaerobic solution of CuCLT in D_2O before (black line) and after (red line) addition of an anaerobic solution containing 15 equiv Angeli's salt in 10 mM NaOD in D_2O.

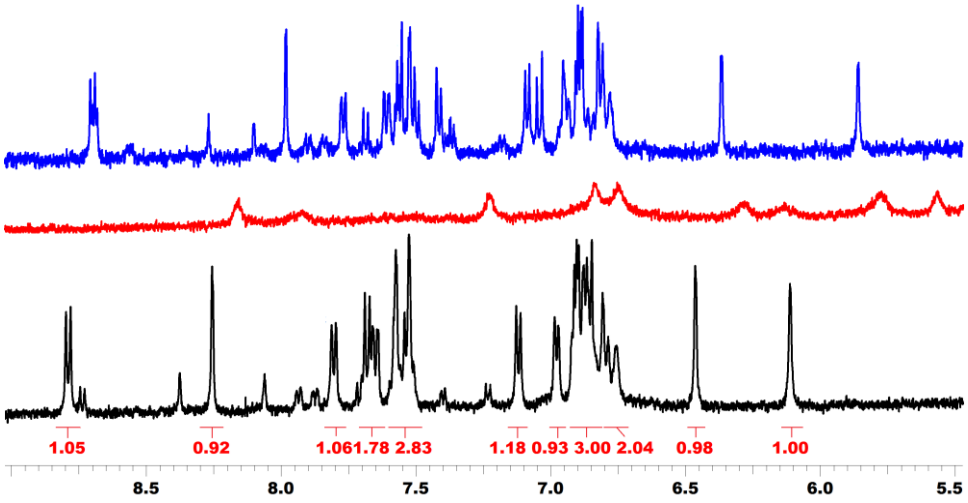

Figure S28. Aromatic region of the ^{1}H NMR spectra of a 1.8 mM solution of QLT in D_2O/CD_3OD = 2:1 (v/v) before (blue line) and after (red line) addition of 0.8 equiv of $CuCl_2$ in D_2O to generate the CuQLT complex. The black spectrum illustrates the sharpening of the resonances upon addition of 20 equiv of L-cysteine in D_2O to the CuQLT solution.

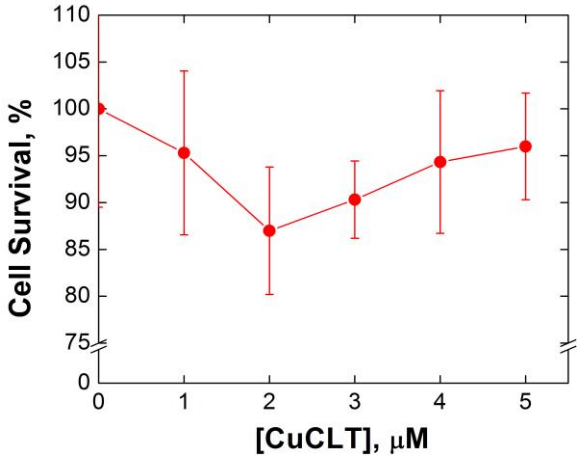

Figure S29. Cytotoxicity of CuCLT applied to HeLa cells treated with different concentrations of the sensor in DMEM growth medium for 24 h, measured by the MTT assay.

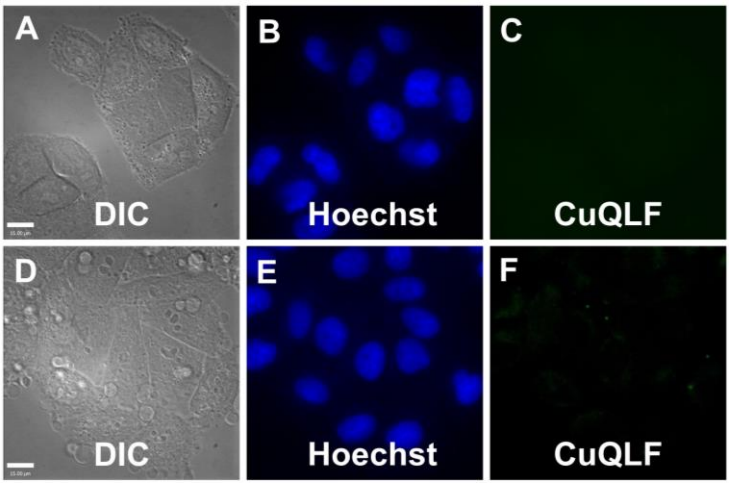

Figure S30. Fluorescence microscopy images of live HeLa cells incubated with 6 μM CuQLF and 15 μM Hoechst 33258 at 37 °C for 30 min in PBS, illustrating cellular impermeability of CuQLF. Top: control cells. (A) Differential interference contrast (DIC) image. (B) Nuclear staining by Hoechst 33258. (C) Signal from CuQLF. Bottom: cells pre-incubated with 1 mM *N*-methylmaleimide (NMM) in PBS for 40 min at 37 °C. (D) DIC image. (E) Nuclear staining by Hoechst 33258. (F) Signal from CuQLF. Scale bar = 15 μm.

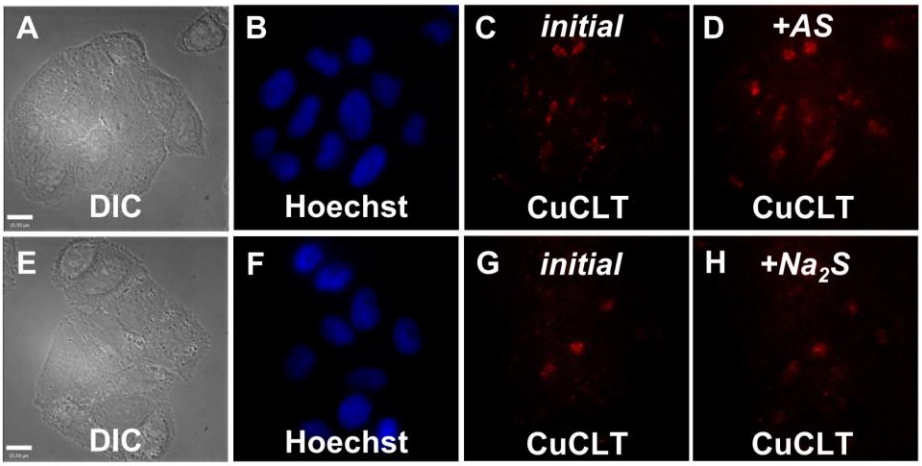

Figure S31. Full-field view of Fig. 7 of the main text. Fluorescence microscopy images of live HeLa cells incubated with 4 μM CuCLT and 15 μM Hoechst 33258 at 37 °C for 15 min in PBS. Top: cells treated with Angeli's salt (AS). (A) DIC image. (B) Nuclear staining by Hoechst 33258. CuCLT signal (C) before and (D) 10 min after treatment with 1.5 mM AS on the microscope stage. Bottom: cells treated with Na_2S. (E) DIC image. (F) Nuclear staining by Hoechst 33258. CuCLT signal (G) before and (H) 10 min after treatment with 1.25 mM Na_2S on the microscope stage. Scale bar = 15 μm.

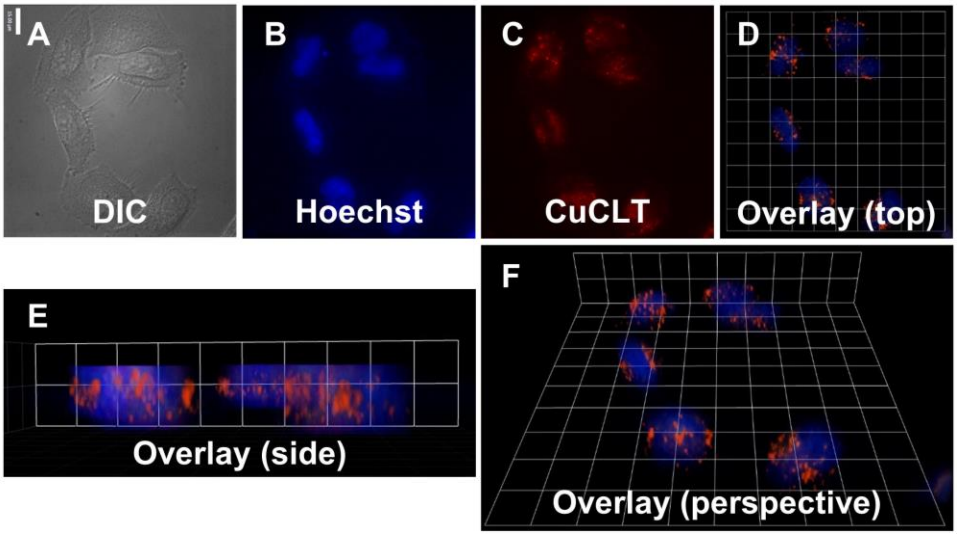

Figure S32. Spatial distribution of CuCLT in live HeLa cells incubated with 4 μM CuCLT and 15 μM Hoechst 33258 at 37 °C for 15 min in PBS. Top: 2D representations down the *Z* axis. (A) DIC image. (B) Nuclear staining by Hoechst 33258. (C) CuCLT signal. (D) Overlay of Hoechst 33258 and CuCLT. Bottom: reconstructed 3D images obtained at different values along the *Z* axis showing the spatial overlap between CuCLT and Hoechst 33258. (E) Side view. (F) Perspective view. Scale bar = 15 μm (A-C). Scale grid = 13 μm (D-F).

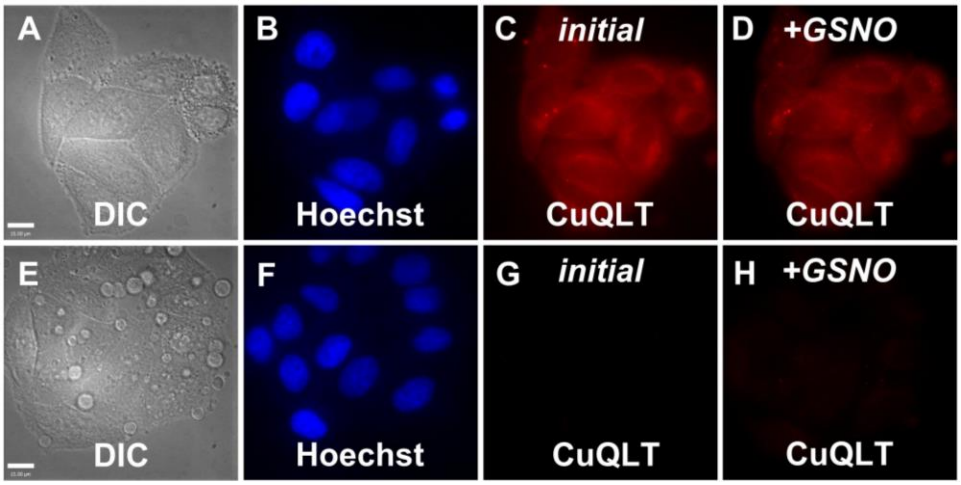

Figure S33. Full-field view of Fig. 11 of the main text. Fluorescence microscopy images of live HeLa cells incubated with 4 μM CuQLT and 15 μM Hoechst 33258 at 37 °C for 15 min in PBS. Top: control cells. (A) DIC image. (B) Nuclear staining by Hoechst 33258. CuQLT signal (C) before and (D) 15 min after treatment with 1.5 mM GSNO on the microscope stage. Bottom: cells pre-incubated with 1 mM *N*-methylmaleimide (NMM) in PBS for 30 min at 37 °C. (E) DIC image. (F) Nuclear staining by Hoechst 33258. CuQLT signal (G) before and (H) 15 min after treatment with 1.5 mM GSNO on the microscope stage. Scale bar = 15 μm.

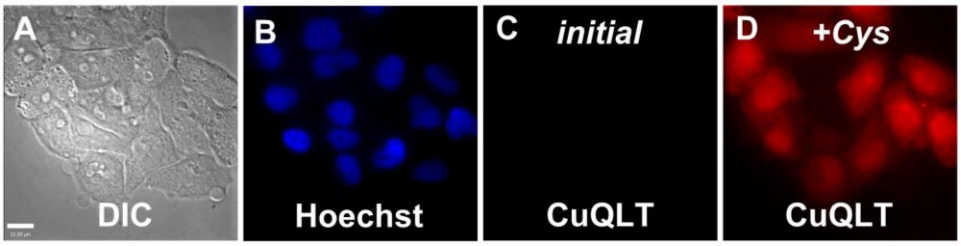

Figure S34. Fluorescence microscopy of live Hela cells pre-incubated with 1 mM *N*-methylmaleimide (NMM) in PBS for 30 min at 37 °C and then incubated with 4 μM CuQLT and 15 μM Hoechst 33258 at 37 °C for 20 min in PBS. (A) DIC image. (B) Nuclear staining by Hoechst 33258. CuQLT signal (C) before and (D) 15 min after treatment with 1.5 mM L-cysteine (Cys) on the microscope stage. Scale bar = 15 μm.

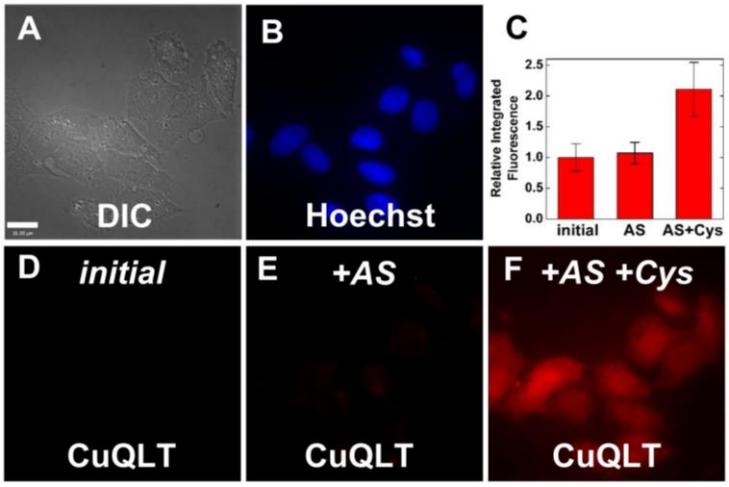

Figure S35. Fluorescence microscopy of live Hela cells pre-incubated with 1 mM *N*-methylmaleimide (NMM) in PBS for 30 min at 37 °C and then incubated with 4 μM CuQLT and 15 μM Hoechst 33258 at 37 °C for 20 min in PBS. (A) DIC image. (B) Nuclear staining by Hoechst 33258. CuQLT signal (D) initially, (E) 10 min after treatment with 1.5 mM Angeli's salt (AS), and (F) 10 min after subsequent addition of 3 mM L-cysteine (Cys) on the microscope stage. (C) Quantification of the intracellular fluorescence response of CuQLT (mean ± SD, N = 48). Scale bar = 15 μm.

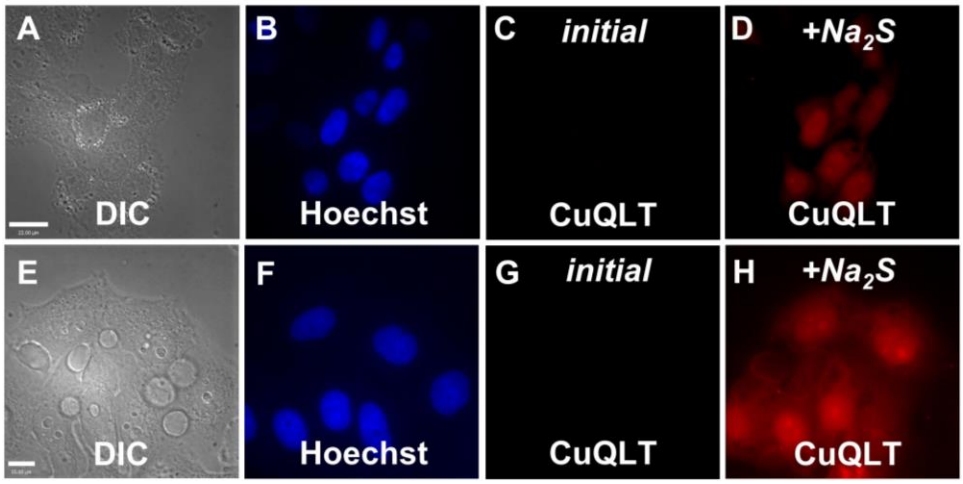

Figure S36. Full-field view of Fig. 12 of the main text. Fluorescence microscopy images of live HeLa cells incubated with 4 μM CuQLT and 15 μM Hoechst 33258 at 37 °C for 15 min in PBS. Top: control cells. (A) DIC image. (B) Nuclear staining by Hoechst 33258. CuQLT signal (C) before and (D) 15 min after treatment with 1.25 mM Na_2S on the microscope stage. Bottom: cells pre-treated with 200 μM DETA NONOate for 20 h at 37 °C in DMEM. (E) DIC image. (F) Nuclear staining by Hoechst 33258. CuQLT signal (G) before and (H) 15 min after treatment with 1.25 mM Na_2S on the microscope stage. Both sets of cells were pre-incubated with 1 mM NMM in PBS for 30 min at 37 °C. Scale bar = 15 μm.

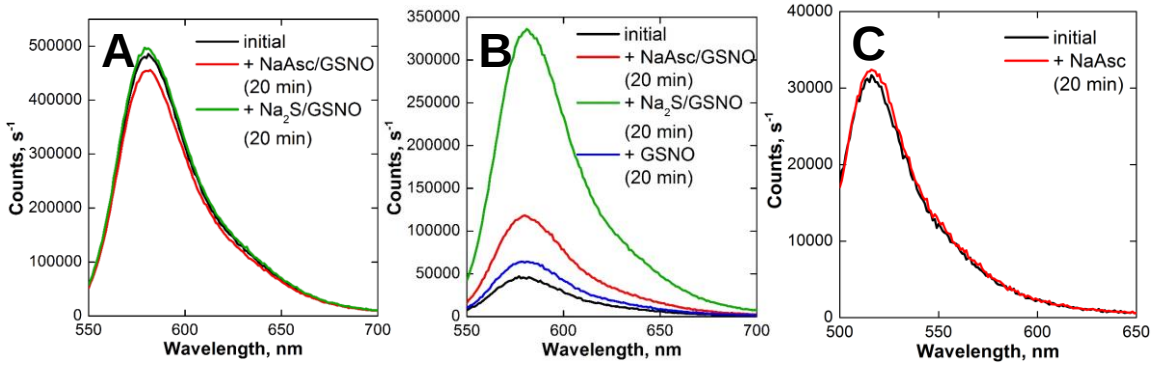

Figure S37. Fluorescence emission spectra of 5 μM solutions of (A) CuCLT, (B) CuQLT, and (C) Cu_2FL2E in aqueous buffer, recorded before and 20 min after addition of 100 equiv of sodium ascorbate and GSNO (NaAsc/GSNO), 100 equiv of sodium sulfide and GSNO (Na_2S/GSNO), or 100 equiv of sodium ascorbate only, respectively (25 °C, 100 mM KCl, 50 mM PIPES, pH 7.0, λ_{ex} = 540 nm for CuCLT and CuQLT, 490 nm for Cu_2FL2E). The blue trace of (B) corresponds to 5 μM CuQLT 20 min after addition of 100 equiv of GSNO only.

References

1. H. E. Gottlieb, V. Kotlyar and A. Nudelman, *J. Org. Chem.*, 1997, **62**, 7512-7515.
2. E. S. Rector, K. S. Tse, A. H. Sehon and R. J. Schwenk, *J. Immunol. Methods*, 1978, **24**, 321-336.
3. C. J. Fahrni and T. V. O'Halloran, *J. Am. Chem. Soc.*, 1999, **121**, 11448-11458.
4. S. C. Burdette, G. K. Walkup, B. Spingler, R. Y. Tsien and S. J. Lippard, *J. Am. Chem. Soc.*, 2001, **123**, 7831-7841.
5. M. V. Kvach, I. A. Stepanova, I. A. Prokhorenko, A. P. Stupak, D. A. Bolibrukh, V. A. Korshun and V. V. Shmanai, *Bioconjugate Chem.*, 2009, **20**, 1673-1682.
6. C. C. Woodroofe, R. Masalha, K. R. Barnes, C. J. Frederickson and S. J. Lippard, *Chem. Biol.*, 2004, **11**, 1659-1666.
7. L. E. McQuade and S. J. Lippard, *Inorg. Chem.*, 2010, **49**, 7464-7471.
8. S. B. King and H. T. Nagasawa, *Methods Enzymol.*, 1999, **301**, 211-220.
9. C. Bueno, M. L. Villegas, S. G. Bertolotti, C. M. Previtali, M. G. Neumann and M. V. Encinas, *Photochem. Photobiol.*, 2002, **76**, 385-390.
10. J. H. Brannon and D. Magde, *J. Phys. Chem.*, 1978, **82**, 705-709.
11. M. H. Lim, D. Xu and S. J. Lippard, *Nat. Chem. Biol.*, 2006, **2**, 375-380.
12. S. Stoll and A. Schweiger, *J. Magn. Reson.*, 2006, **178**, 42-55.
13. M. Kirsch, A. M. Buscher, S. Aker, R. Schulz and H. de Groot, *Org. Biomol. Chem.*, 2009, **7**, 1954-1962.